Bernardo Luís Moura Mendes

Bachelor in Micro and Nanotechnologies Engineering

Electronic textiles functionalized with conductive polymers

Dissertation submitted in partial fulfilment of the requirements for the degree of
Master of Science in
Micro and Nanotechnology Engineering

Advisor: Dr. Ana Catarina Bernardino Baptista, Researcher at CENIMAT/I3N, Faculty of Sciences and Technology, NOVA University of Lisbon

Co-advisor: Dr. Bruno Miguel Morais Faustino, Post-doctoral researcher, Faculty of Sciences and Technology, NOVA University of Lisbon

Examination Committee:

Chair: Dr. Luís Miguel Nunes Pereira, Associate Professor, NOVA University of Lisbon

Rapporteurs: Dr. Joana Dória Vaz Pinto, Invited Assistant Professor, NOVA University of Lisbon

Members: Dr. Ana Catarina Bernardino Baptista, Researcher, NOVA University of Lisbon

FACULDADE DE CIÊNCIAS E TECNOLOGIA
UNIVERSIDADE NOVA DE LISBOA

October, 2019

Electronic textiles functionalized with conductive polymers

“Waste no more time arguing what a good man should be. Be One.”

-Marcus Aurelius, *Meditations*

Acknowledgement

Em primeiro lugar quero expressar os meus agradecimentos a esta instituição, a Faculdade de Ciências e Tecnologia da Universidade Nova de Lisboa, por me ter dado este espaço que nos últimos anos foi uma segunda casa para mim. É com carinho que demonstro a minha gratidão a todos os professores e colegas que me permitiram fazer a tese no DCM, onde aprendi bastante. Gostaria de começar por agradecer pessoalmente à professora Isabel Ferreira por me ter dado a oportunidade de realizar a minha dissertação neste espaço, à minha orientadora, a professora Ana Baptista e a sua imensurável paciência neste processo, tal como o meu co-orientador, Bruno Miguel. A todos os meus colegas de trabalho no DCM que sempre se mostraram disponíveis: ao David, Nuno, Jaime, Ana Maques, Ana Gaspar, Ana Pinheiro, Ricardo, Patrícia, Sofia e à Ana, que apesar de já não se encontrar no DCM foi essencial para que pudesse fazer a caracterização piezoresistiva na minha dissertação e que se mostrou sempre disponível a ajudar-me a compreender melhor o Arduíno.

Não posso deixar de agradecer ao professor Rodrigo Martins e à professora Elvira Fortunato, pois sem a sua ajuda não seria possível graduar-me num curso de tanto interesse e aprendizagem que foi a minha aventura no mestrado integrado em Micro e Nanotecnologias.

Um agradecimento especial ao professor João Pedro Oliveira e aos seus alunos do departamento de engenharia mecânica por terem ajudado com os testes de abrasão.

Trazendo os agradecimentos para as pessoas mais perto de mim, começo por agradecer às duas famílias que formei na faculdade: ao Nuno, Pedro, Tomás, Zé, Luka, Miguel, Sofia, Joana e Carolina e ainda aos mais novos que me acompanharam de perto nestes últimos dois anos e que me surpreenderam com todo o seu apoio e forma de encarar as dificuldades: ao Pedro, Catarina, Laura, Xavier e Gonçalo.

Aos meus amigos mais perto, eles sabem que sou sempre o reflexo das nossas ações e das nossas atitudes perante o mundo. Ao Diogo e ao Tiago por serem as pessoas empáticas e determinadas que são, e pela forma como sempre foram influenciando positivamente a minha vida. Ao Pedro Barata, cujo ajuda fundamental a conceber modelos 3-D fez dele merecedor de dois nomes nestes agradecimentos, ao Nuno pela miríade de conversas que me fez compreender melhor a minha pessoa, merecendo uma palavrinha cara, ao Diogo, que ajudes a salvar todos os bichos do mundo e a dar-lhes o respeito que a ignorância humana nem sempre atinge, à Margarida que tem sido a pessoa que mais cresceu comigo nos últimos anos e que todos os dias me impressiona e apoia, ao Pedro por ser sempre um dos meus maiores apoios, e por fim à Carlota, que todas as discórdias sejam um símbolo que representa o respeito em opiniões diferentes. A todos aqueles que tiraram um bocado do seu dia para ouvir as minhas queixas e que me deram sugestões neste percurso.

Para o fim deixo o mais importante, os meus pais, que sempre deram grande parte de si para a minha educação enquanto pessoa, aluno e cidadão. Eles moldaram as partes mais importantes de mim, a minha empatia e a minha determinação para concretizar algo, o que quer que isso signifique para mim.

Abstract

Smart textiles have received a lot of attention nowadays for combining two of the most prolific industries: fabrics and electronics. This was possible due to the evolution of conductive polymers, meaning that a material as conductive as metals with flexible properties was in the market. Its potential to integrate signals and stimuli from contact means that a myriad of applications might be in the making, spanning interest from electronics to communication, military and biomedical uses.

The main goal of this work was to study different methodologies to functionalize commercial textiles with conductive polymers to obtain piezoresistive textiles.

Polypyrrole (PPy) and poly(3,4-ethylenedioxythiophene) (PEDOT) are two intrinsically conductive polymers used to functionalize lycra and felt textiles. Such functionalization was carried out by in situ-polymerization of pyrrole (Py) and 3,4-ethylenedioxythiophene (EDOT). Several polymerization conditions were evaluated to determine the most suitable ones to prepare stable conductive textiles. In-plane electrical conductivities of 6.707x10^{-3} Scm^{-1} to 1.808x10^{-2} Scm^{-1} and transversal conductivities of 1.837x10^{-4} Scm^{-1} to 2.040x10^{-3} Scm^{-1} were reached throughout textiles.

Morphological, chemical and electrical characterization was carried before and out after polymerization.

Piezoresistive behaviour of textiles was studied, because coated and agglomerated polymer comes into different contacts when stress is applied. Two different approaches were studied: stretch behaviour for elastic lycra ranging from 11-26kΩ and pressure behaviour for felt textiles ranging from 0.72-19.54kΩ.

Finally, stability tests were studied. In this section, abrasion was performed to show the wear off textiles. Felt had the best stability with values from 3.903x10^{-4} $S.cm^{-1}$ to 6.685x10^{-6} $S.cm^{-1}$, while lycra had the worst results, from 1.242x10^{-4} $S.cm^{-1}$ to 2.696x10^{-11} $S.cm^{-1}$. Conductivity over time was studied, showing there is over a 50% conductivity decline over 6 months. Washing cycles, showed declines of over four orders of magnitude, compromising further use.

Keywords: Polypyrrole, PEDOT, smart textiles, piezoresistive, flexible electronics.

Resumo

Os têxteis inteligentes têm recebido atenção nos últimos anos por combinarem duas das indústrias mais prolíficas: têxteis e eletrónica. Tal foi possível devido à evolução de polímeros condutores, materiais com propriedades condutoras como os metais, mas flexíveis. O seu potencial para integrar estímulos através de contacto significa que muitas aplicações na área de eletrônica a comunicação, militar e biomédicas possam surgir.

O objetivo principal deste trabalho consistiu em estudar diferentes metodologias para funcionalizar têxteis comerciais para obter aplicações piezoresistivas através de polímeros condutores.

Polipirrol (PPy) e poli(3,4-etilenodioxitiofeno) (PEDOT) são dois polímeros condutores intrínsecos, usados para funcionalizar textêis de lycra e feltro. Foi utilizada polimerização *in situ* do pirrol (PY) e do 3,4- etilenodioxitiofeno (EDOT). Várias condições foram estudadas com o objetivo de avaliar o melhor procedimento para obter têxteis estáveis. Condutividades planares de 6.707x10^{-3} Scm^{-1} a 1.808x10^{-2} Scm^{-1} e tranversais de 1.837x10^{-4} Scm^{-1} a 2.040x10^{-3} Scm^{-1} foram obtidas nos tecidos.

Caracterizações morfológicas, químicas e elétricas foram estudadas antes e depois de polimerizações.

O comportamento piezoresistivo das amostras foi estudado, devidos ao revestimento e aglomerados gerados pela polimerização que entram em contacto quando forças são aplicadas. Dois comportamentos foram estudados: extensão dos tecidos elásticos de lycra, obtendo valores de 11-26kΩ e pressão do feltro, obtendo valores de 0.72-19.54kΩ.

Finalmente, testes de estabilidade foram executados. Abrasão para observar o dano às fibras, de 3.903x10^{-4} $S.cm^{-1}$ a 6.685x10^{-6} $S.cm^{-1}$ para o feltro, que teve os melhores resultados, enquanto lycra teve resultados de 1.242x10^{-4} $S.cm^{-1}$ a 2.696x10^{-11} $S.cm^{-1}$. Condutividades ao longo do tempo também foram estudadas, mostrando baixas na condutividade acima dos 50% ao longo de 6 meses. Ciclos de lavagem foram realizados, obtendo condutividades até quatro ordens de grandeza abaixo das iniciais, comprometendo o uso dos têxteis.

Palavras-chave: Polipirrole, PEDOT, têxteis inteligentes, piezoresistividade, eletrônica flexível.

Abbreviations

E-textile	Electronic textile
ECP	Extrinsic conductive polymer
EDOT	3,4-ethylenedioxythiophene
EDS	Energy-dispersive X-ray spectroscopy
GF	Gauge factor
ICP	Intrinsic conductive polymer
IPA	Isopropanol
PANI	Polyaniline
PDCY	Composite made of polyurethane and polyester
PE	Polyester
PEDOT	Poly(3,4-ethylenedioxythiophene)
PPy	Polypyrrole
PSS	Poly(styrene sulfonic acid)
PU	Polyurethane
Py	Pyrrole
Raman	Raman spectroscopy
SEM	Scanning Electron Microscopy
ZnO NW	Zinc oxide nanowire
rGO	Reduced graphene oxide

Symbols

A	area
I	current
d	length of electrode
L	distance between electrodes
l	width of electrode
R	resistance
S	sensitivity
rpm	rotations per minute
µm	micrometer (thickness)
Ɛ	elongation
ρ	resistivity
σ	conductivity

Table of Contents

1 Introduction 1
1.1 Smart textiles 1
1.1.1 Evolution 1
1.2 Conductive polymers 2
1.2.1 History of conductive polymers 2
1.2.2 Polypyrrole 3
1.2.3 PEDOT 3
1.3 Piezoresistive behaviour 5
2 Materials and Methods 6
2.1 Textile preparation 6
2.2 Textile functionalization: in situ oxidative polymerization 6
2.2.1 Py polymerization: 6
2.2.2 EDOT Vapor-phase polymerization 6
2.3 Textile characterization 6
3 Results and Discussion 8
3.1 Textile characterization 8
3.2 Electrical characterization 9
3.2.1 Polypyrrole conductivity 11
3.2.2 PEDOT conductivity 13
3.3 Morphological characterization 15
3.3.1 SEM 15
3.3.2 Raman spectroscopy 17
3.4 Piezoresistive characterization 19
3.4.1 Fatigue traction tests 19
3.4.2 Pressure tests 22
3.5 Stability tests 24
3.5.1 Abrasion tests 24
3.5.2 Washing cycles 27
3.5.3 Conductivity over time 28
Conclusion and Future Perspectives 29

List of Figures

Figure 1.1- Smart clothing shipments worldwide, statista. 1

Figure 1.2- Polypyrrole structure. 3

Figure 1.3- PEDOT structure. 4

Figure 1.4- Illustration of applied forces to textiles. A) lycra; B) Felt. 5

Figure 2.1-Visual representation of the applied forces to textiles. a) stretch on lycra textiles and b) pressure on felt textiles. 7

Figure 3.1-Macro- and microscopic morphology of lycra and felt textiles. 8

Figure 3.2- Visual representation of the dimensions used for conductivity tests. left- transversal; right- planar. 11

Figure 3.3-Conductivities of lycra textiles polymerized with PPy, The y-class represents conductivity in S.$cm-1$, while the x-class represent the times. On the bottom are represented the polymerization synthesis times in min, while on top are represented the annealing's´: 0 represents the sample drying at ambient temperature, while 24 and 48 are the hours spent in annealing at 60˚ C. a) transversal tests; b) planar tests. 11

Figure 3.4-Conductivities of felt textiles polymerized with PPy, The y-axis represents conductivity in S.cm^(-1), while the x-axis represent the times. On the bottom are represented the polymerization synthesis times in min, while on top are represented the annealing's´: 0 represents the sample drying at ambient temperature, while 24 and 48 are the hours spent in annealing at 60˚ C. a) transversal tests; b) planar tests. 12

Figure 3.5-Conductivities of lycra textiles polymerized with PEDOT. The y-axis represents conductivity in S.$cm-1$, while the x-axis represents the times in minutes. a) transversal tests; b) planar tests. 13

Figure 3.6 -Conductivities of felt textiles polymerized with PEDOT. The y-axis represents conductivity in S.$cm-1$, while the x-axis represents the times in minutes. a) transversal tests; b) planar tests. 14

Figure 3.7-SEM images of polymerized textiles. 16

Figure 3.8-Raman spectroscopy of PPy polymerized samples: a) Lycra; b) felt. 17

Figure 3.9--Raman spectroscopy of PEDOT polymerized samples. a) Lycra; b) felt. 18

Figure 3.10-Assembly of stretch-strain test machine. 20

Figure 3.11-Stretch tests on lycra-PPy textiles. a) 10 cycles; b) 300 cycles. 20

Figure 3.12-Stretch tests on lycra-PEDOT textiles. a) 10 cycles; b) 300 cycles. 21

Figure 3.13-Assembly of pressure strain test machine. 22

Figure 3.14-Felt-PPy pressure tests. a) low pressure; b) high pressure. 23

Figure 3.15-Felt-PEDOT pressure tests. a) low pressure; b) high pressure. 23

Figure 3.16-Visual representation of abraded textiles with controlled times:0, 2:30 and 5 hours. a) lycra-PPy; b) lycra-PEDOT; c) felt-PPy; d) felt-PEDOT.....25

Figure 3.17- Planar conductivity of abraded lycra samples. a) PPy; b) PEDOT. 26

Figure 3.18-Planar conductivity of abraded felt samples. a) PPy; b) PEDOT.....26

Figure 3.19- Transversal conductivity after washing cycles of lycra samples. a) PPy; b) PEDOT.....27

Figure 3.20- Transversal conductivity after washing cycles of felt samples. a) PPy; b) PEDOT. 27

Figure 3.21-Visualization of conductivity decline over 6 months: a) transversal, b) in-plane.....28

List of Tables

Table 1.1- State of the art for e-textiles in novel technologies 4

Table 3.1- Textiles physical properties before polymerization. 9

Table 3.2- PPy synthesis parameters 9

Table 3.3- Optimal lycra-PPy conductivity and resistivity values.....12

Table 3.4-Optimal felt-PPy conductivity and resistivity values. 13

Table 3.5-Optimal lycra-PEDOT conductivity and resistivity values. 14

Table 3.6-Optimal felt-PEDOT conductivity and resistivity values.....15

Table 3.7-Band assignments for Raman spectra of PPy at λ=533 nm 18

Table 3.8-Band assignments for Raman spectra of PEDOT at λ=533 nm. 19

Table 3.9-Fatigue traction test metrics. 22

Table 3.10-Pressure tests metrics. 24

Motivation and objectives

Flexible electronics receive a lot of attention nowadays, as the next step in electronics, mainly due to their lightweight properties and flexibility. Conductive polymers appeared as a good candidate for electronic applications more than 40 years ago, since they have high conductivity, ranging between semiconductor and metal values. Intrinsically conductive polymers (ICPs) such as polypyrrole (PPY) and poly(3,4-ethylenedioxythiophene) (PEDOT), are some of the most widely used polymers, due to their high conductivity, high stability and ease of preparation.

Their biocompatibility is also an advantage. Since this work addressed textiles for clothing purposes, no toxic effects to human skin should be observed. Polypyrrole and PEDOT showed to be biomedical viable, having *in vivo* and *in vitro* properties, with applications such as nerve grafts, heart muscle patches, blood conduits or neural probes.

Even though these materials show high conductivity and biocompatibility, some challenges still lay in the path of organic materials in electronics. Most notably, brittleness, mechanical rigidity and insolubility after processing, making their process a very delicate one, and as such, the conditions to manufacture millions of units yearly require good processability.

The main purpose of this dissertation is to study methodologies to functionalize commercial textiles with ICPs that are less expensive and easy-to-use to obtain piezoresistive sensors. The behaviour of electrical resistance when stress is applied will be studied, not as a finalized sensor, but to understand its viability in today´s market.

Functionalized textiles will be studied in this work, from the conditions of the synthesis, to conductivity values, and then, after selecting the best samples, morphology, electrical and stability tests will be performed, to evaluate whether these textiles are suitable for electronic textiles. Finally, strategies to improve the performance of both methods and mode of operation will be studied as well.

1 Introduction

1.1 Smart textiles

Smart, or e-textiles (derived from electronic textiles), are a group of specially made fabrics that can sense, respond and adapt to internal or external stimuli and changes in the environment by integrating functionalities to textile structure [1], [2].

There are different purposes for e-textiles. While commercially, these are mostly known for fashion, interactive and fun purposes such as light patterns embroiled in clothes [3], this thesis focus on the performance-enhancing factors which improve an action in a more easily and controlled way than what would be conducted without it.

1.1.1 Evolution

Smart materials have been studied for some decades, starting around 1960 with the discovery of shape materials, and later in the '70s with intelligent polymeric gels.

Whilst the concept of smart textile was defined for the first time in Japan around 1989 over a silk thread having shape memory, the concept has evolved far beyond that point. With important milestones such as communicative textiles in the '90s and textile electronic semiconductive components in the early 2000s, and the present situation is even more dynamic. Their applications span from medical components to transportation and energy, and even in the areas of military, security, communication, and electronics [1], [2].

While predicting the future is an ever evolving and challenging task, it is expected that smart textiles will evolve in two ways. The first one could be low-cost, and it would be mainly mass-produced clothes, home, transportation or infrastructure textiles. The second one would seek dedicated uses and should be more valuable and harder to produce, mainly in medical, security and research areas.

Nowadays, e-textiles face steady value growth. In 2016, it has been reported that the value of 1kg of technical textiles was estimated at US$5.3 compared to US$3.4 for nonwoven textiles, and US$10.5 for composite textiles [1]. Not only is the price growing, but also the market search, as estimated in Figure 1 [4].

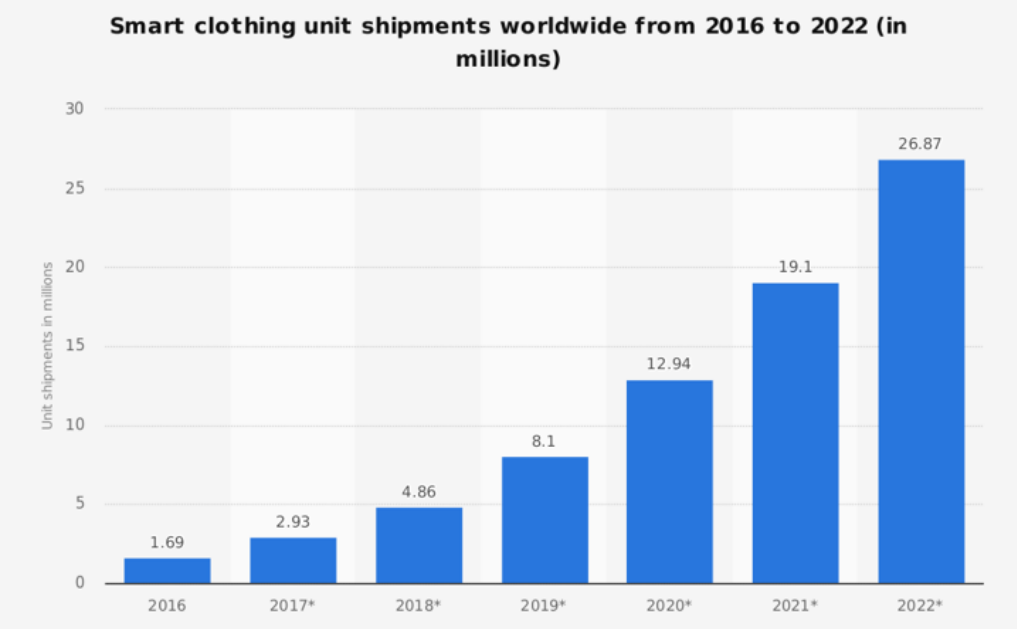

Figure 1.1- Smart clothing shipments worldwide, statista.

The work presented seeks not only to bridge the connection between textiles and electronics, but also to pave the way for e-textiles to be used as sensors, possibly connecting to batteries or even integrate with signals such as wi-fi, since the upcoming upgrade to WiFi 6 (802.11ax) means more connected devices in real-time, a much-desired application in the areas of medicine, sports, military, communications, and even security and fraud.

In this thesis, a combination of two different textiles with two conductive polymers were studied to produce piezoresistive sensors. For the textiles, commercial lycra and felt were used. Lycra is a highly stretchable and organized interwoven fabric with low thickness. Felt, on the other hand, is a fabric with high thickness, randomly orientated fibres, and high swelling behaviour. The composite materials result in a piezoresistive behaviour.

1.2 Conductive polymers

While the definition of a conductive polymer is not clearly defined, according to IUPAC, or International Union of Pure and Applied Chemistry, a polymer is “a molecule of high relative molecular mass, the structure of which essentially comprises the multiple repetition of units derived, actually or conceptually, from molecules of low relative molecular mass” [5], [6]. In this explanation, some words such as high, low and multiple are not very precise, but it helps to understand how the name derives from the open definition of the conjugation of the Greek words “poly” (many) and “mer” (parts).

Another divergence rests on the fact that the complete term presented, can also be misunderstood, because there are two different meanings in scientific literature. The blends of electrically conductive additives, like metallic fibres or carbon in its graphite modification, such as nanotubes, with duromers or thermoplastic polymers, sometimes are denoted as conductive. These polymers refer to the extrinsically conductive polymers since the material itself behaves as an insulator. This work deals only with intrinsically conductive polymers (ICPs) [6]. ICPs are organic materials with extended π-conjugation along the molecular backbone, and their conductivity can be changed by several orders of magnitude, from a semiconducting state to a metallic state, via doping. Usually, p-doping is achieved by partial oxidation of the polymer by a chemical oxidant or an electrochemical method and causes depopulation of the bonding π orbital (HOMO), with the formation of holes. In addition to applications in organic printable electronics, such as organic light-emitting diodes (OLEDs) and organic photovoltaic (OPV) solar cells, ICPs find use in charge dissipating (antistatic) layers, conducting composites and chemical research [5]–[7].

1.2.1 History of conductive polymers

The story of ICPs states back to 1862, when H. Letheby, studied the behaviour and chemical reactions of aniline. He did so after the death of two people,victims of poisoning by nitrobenzene, where aniline had been found as a metabolite, in their stomach [6].

Through electro polymerization of aniline sulfate to a bluish-black solid layer on a platinum electrode, Letheby studied and published his findings in the Journal of the Chemist Society. At the time, the chemical reactions that gave colour to products remained unknown. It was only in 1977 that the biggest breakthrough that gave space to conductive polymers in research happened when doped polyacetylene was discovered and published. The finding consisted of the conjugation of hydrocarbon (CH)x, combined with halogens, to obtain high conductivities through doping. This novel research earned Alan J. Heeger, Hideki Shirakawa, and Alan G. MacDiarmid the Nobel prize in 2000 [6], [8], [9].

Nowadays, there are over 25 conductive polymer systems. They merge the positive properties of metals and conventional polymers, not just the ability to conduct charges, but also great electrical and optical properties, with flexibility in processing and ease of synthesis [6]. Conductive polymers can be prepared mainly through two methods: chemical synthesis and electro-polymerization. The former is done by connecting C-C bonds of monomers, by placing these under various situations conditions, such as heating, pressing, light exposure and catalysts. Their main advantage is their high yield, unfortunately

producing many impurities. The later method generally means inserting three electrodes (reference, counter, and working) into a solution that has reactors or monomers. A redox reaction occurs by applying voltage to the electrodes that promote the synthesis of the polymer. This method is further divided into cyclic voltammetry and potentiostatic, whether a cyclic or constant voltage is applied, respectively. Electro-polymerization´s advantages are high purity of electrodes, even though their yield is low [10].

On this thesis, two polymers, Polypyrrole (PPy) and poly(3,4-ethylenedioxythiophene) (PEDOT) were prepared by *in situ* chemical oxidative polymerization.

1.2.2 Polypyrrole

Probably the most studied conductive polymer, PPy possesses high conductivity once oxidized, environmental stability, and stimulus-responsive properties, making it a promising "smart" biomaterial.

Between the discoveries of the first conductive polymer, polyaniline, and it´s conductivity, PPy was researched by D.E. Weiss and colleagues in Australia, around the early 1960s. Their work described the thermolysis of tetraiodopyrrole, reaching a conductivity of 1S/cm. In the years of 1968/1969, Dall´Olio and coauthors oxidized pyrrole to polypyrrole. This study, based on the method of electro polymerization surpassed the previous work, and a conductivity of 7.54S/cm was found, at ambient temperature. They also noted that while PPy films are yellow, they darken into a black colour once oxidized [6].

Most importantly, since this work revolves on conjugating textiles and conductive polymers, a material capable of being biocompatible is necessary, making PPy a very good candidate, since it has good *in vitro* and *in vivo* biocompatibility, good chemical stability, and its conductivity remains high under physiological conditions. Another reason why polypyrrole was picked for this thesis is its synthesis. PPy can be easily and flexibly synthesized in large quantities at room temperature in a wide range of solvents, including water, allowing for low-cost fabrication, especially via chemical polymerization, which was the used method, using an oxidizing agent. Nevertheless, it can also be produced by electrochemical polymerization [6], [11], [12].

It can be fabricated with large surface areas, different porosities and modified for more biomedical applications through the incorporation of bioactive molecules. Since it is stimulus-responsive, it´s properties can be dynamically controlled by applying an electrical potential [6], [12].

Polypyrrole has many applications, such as cells ´fuel, corrosion protection, computer displays, microsurgical tools, biosensors and drug delivery systems, neural tissue engineering, neural probes, nerve guidance channels, and blood conduits [8], [11]–[20].

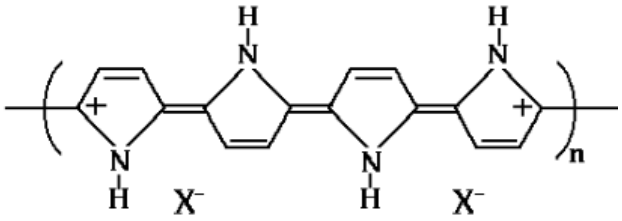

Figure 1.2- Polypyrrole structure.

1.2.3 PEDOT

Formed by the polymerization of the bicyclic monomer 3,4-ethylenedioxythiophen (EDOT), PEDOT is a conjugated polymer with a dioxyalkylene bridging group across its 3rd and 4th positions of the heterocyclic ring, resulting in a lower band gap, lower redox potential, high stability, and optical transparency. These characteristics are also better than polythiophene (PTh), the polymer it derives from.

PEDOT´s invention started around 1980, when Bayer´s Central Research Department, focused on polyacetylenes to achieve processability of these polymers in their highly doped form. Ultimately, the

attempt failed, but it didn´t stop the company from branching its research on other conductive polymers, such as polypyrrole and polythiophenes. Followed by failure in stabilizing thiophene structures with oxygen substitutes, due to destruction of samples when placed in contact with humid air, the research was extended to bicyclic ring molecules. This attempt too, started unsuccessfully, when decarboxylation (the chemical reaction that removes a carboxyl group, releasing) failed. The breakthrough came with the electrochemical polymerization of EDOT, using as oxidant, achieving high conductivity and stability. A week later, the use of PEDOT in capacitors was filed by the investigators in the German company, becoming one of the largest applications ever. The company upgraded the commercial use of the polymer as well, by using poly(styrene sulfonic acid) (PSS) as a counterion for positively charged PEDOT, circumventing the insolubility problem of the material during in situ polymerization. This new complex is the widely used PEDOT: PSS [6], [21].

Nowadays, PEDOT is used in biosensing and bioengineering applications, neural electrodes, nerve grafts, heart muscle patches, and many electronic ends, such as solid electrolyte capacitors, printed wiring boards, antistatic coating, electroluminescent lamps, OLEDs, solar cells, electrochromic and organic field-effect transistors [3], [6], [21]–[23].

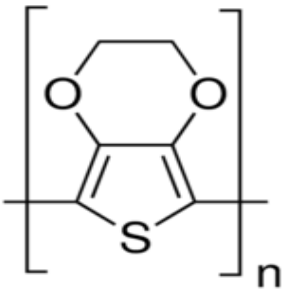

Figure 1.3- PEDOT structure.

Table 1.1- State of the art for e-textiles in novel technologies

Fabrication method	Type	Stretchable component	Sensing component	Sensing range	Gauge factor (GF)	Linearity and hysteresis
In situ chemical polymerization [13]	Fabric	Lycra	PPy	Up to 60%	~-3.5 (20% strain) ~-0.7 (60% strain)	Non-linear Low hysteresis
In situ chemical polymerization [23]	Fibre	Polyester	PEDOT	Up to 20%	~-0.76	Non-linear High hysteresis
Dip-coating [3]	Fabric	Spandex	PEDOT:PSS	Up to 80%	N/A	Non-linear High hysteresis
Vapor phase polymerization [25]	Fibre	Lycra	PPy	Up to 100%	~75 (40% strain) -20 (100% strain)	Non-linear N/A
In situ chemical polymerization [26]	Fibre	PU	PANI	Up to 1500%	~3 (400% strain)	Non-linear High hysteresis
Dip-coating [27]	Yarn	PDCY (PU/PE)	rGO	Up to 200%	~10 (1% strain) ~3.7 (50% strain)	Non-linear High hysteresis

Hydrothermal growth [28]	Fibre	PU	ZnO NW	1.8%-150%	~15.2 (<10% strain) ~4.1 (10-150% strain)	High linearity (10-150% strain) High hysteresis
Non-elastic conducting fibre [29]	Fibre	N/A	Carbon fibre	Up to 1.2%	~2 (1% strain)	High linearity (1% strain) N/A

Table *1.1* describes the state of the art of e-textiles with current technology as well as some metrics used to characterize them [24].

1.3 Piezoresistive behaviour

Piezoresistance is described as the change in electrical resistance in the material by applying mechanical stress [30]. In other words, measuring the electrical resistance while physically inciting responses, like push, pulling, pressing, twisting or other stimuli will prove how well does a textile functionalize with ICPs work when compared with conventional technologies. This effect has been studied often with conventional semiconductors in bulk, such as Silicon technologies, but gained more attention in studies where nanostructures, such as nanowires, have been reported to show over two orders of magnitude of piezoresistive properties 'values above bulk Silicon structures [30].

Gauge factor (GF), describes relative resistance change per unit strain, given by:

$$GF = \frac{dR/R_0}{\varepsilon} \approx \frac{d\rho/\rho_0}{\varepsilon} + 1 + 2\nu \quad (1)$$

Where R_0 and R are the resistance values of the composite (initial and in real time, respectively), dR is resistance change caused by the variation in length ε, or strain, ρ_0 and ρ are the resistivity values (initial and real-time, respectively), and ν is the Poisson ratio. The GF has contributions from the intrinsic piezoresistive effect ($\frac{d\rho/\rho_0}{\varepsilon}$) and the geometrical effect (1 + 2ν) [30], [31]. Conventional gauge factors in metals range from 2-5, while PPy typically ranges from 2 to 3, and PEDOT´s values range from -5 to -20, depending on the applications [2], [24].

Two types of mechanical stress were applied, as presented in Figure 1.4. In accordance with tested textile. Lycra, on one hand, was used as a sensor capable of changing its electrical resistance when strain is applied. This stimulus was applied unidirectionally in the preferred orientation of the fibres, producing the least possible electrical resistance when highly stretched. Felt, on the other hand, is based on pressure being the applied stimulus, reducing the space between fibres, and therefore increasing the points of contact, reducing its electrical resistance.

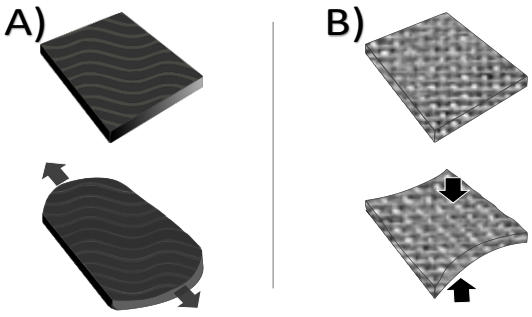

Figure 1.4- Illustration of applied forces to textiles. A) lycra; B) Felt.

2 Materials and Methods

2.1 Textile preparation

Lycra and felt commercial textiles were cut in a rectangular shape (3.0x2.0 cm) and washed with a mixture of water and soap, to remove any impurities on the textile, and then washed again with iso-propanol (IPA) and the left to dry.

2.2 Textile functionalization: in situ oxidative polymerization

2.2.1 Py polymerization:

Textiles were immersed for 10 min, at 100 rotations per minute (rpm) in an oxidant-impregnating solution of $FeCl3.6H_2O$ (Sigma Aldrich, reagent grade ≥98%) - 0.135 g in 10 mL of water. Then, the monomer solution was gently added to the previous solution - 69 µL of pyrrole in 10 mL of water (Sigma Aldrich, reagent grade ≥98%). The oxidant-to-monomer mass ratio was considered constant at 2:1. Different polymerization periods, annealing times and temperature were evaluated. Samples were left to dry at room temperature and 60˚C for 24 and 48 hours.

After the polymerization, the textile was washed with water and ethanol, in order to remove any by-products or unreacted residues of polymerization.

2.2.2 EDOT Vapor-phase polymerization

Firstly, the textiles were immersed in an aquose-solution of $FeCl_3.6H_2O$ – 0.4 g in 20 mL of water. The textile was then left to dry at room temperature for over a day. After that, the textiles were fixed in the top of a closed chamber containing a diluted solution of EDOT (Alfa Aesar, 97%) - 0.5 mL of EDOT in 0.5 mL of water. The sample was then taken to an oven at 80˚C for different polymerization times (30, 90, 180 and 300 minutes).

2.3 Textile characterization

Textiles before and after functionalization with conductive polymers were morphological characterized using a tabletop microscope TM4000 Plus from Hitachi.

Confocal Raman spectrophotometer (Witec Alpha 300 RAS) using a laser with a wavelength (λ) of 533 nm and 1 mW of power was used to analyse the chemical composition of the textile surface.

Electrical conductivities of functionalized textiles were determined from the linear I-V plot using transversal and in-planar configuration. The effect of polymerization conditions on electrical conductivities of samples was also studied in detailed. All electrical measurements were repeated thrice. Transversal and in-plane conductivities were studied. For the later, acetate masks were needed, and therefore designed to “paint” contacts using carbon ink (Appendix A).

Both textiles, coated with PPy and PEDOT were submitted to several washing cycles (10 times) in order to understand if the coating is stable and suitable to be used in daily cloth purposes. The cycles were conducted for 30 min each at 200 rpm, using 100 mL of water and 200 µL of commercially available detergent. Electrical properties were evaluated after each washing cycle.

Additionally, resistance of the functionalized textiles to abrasion was investigated. Abrasion is the physical destruction of fibres, yarns, and fabrics, resulting from the rubbing of a textile surface over another surface. The tests were conducted using glue to fix the textiles to a polymer base and friction was conducted with pig skin, to simulate abrasion between textile and human skin. The tests were conducted over 5 hours, using 17 rpm, with 2 passages on each cycle (Appendix B), totalling 10,200 cycles. Photos were taken at 3 different times (before abrasion, at 2:30 h and 5 h).

Textiles were finally tested as piezoresistive sensors. The electrical resistance of functionalized lycra textiles was evaluated during dynamic tests changing from stretching to relaxing states. Distance was kept as 5 mm for 10 cycles, resulting in a strain of around 17%. A longer test of 300 cycles with the same strain deformation was performed to understand the effect of strain fatigue on the polymerized textile.

Felt functionalized textile were subjected to different pressing forces in the low (1 Pa) and medium regime (90 KPa) while electrical resistance was evaluated.

Figure 2.1 offers a visual representation on the types of forces that were applied, to characterize textiles as piezoresistive sensors.

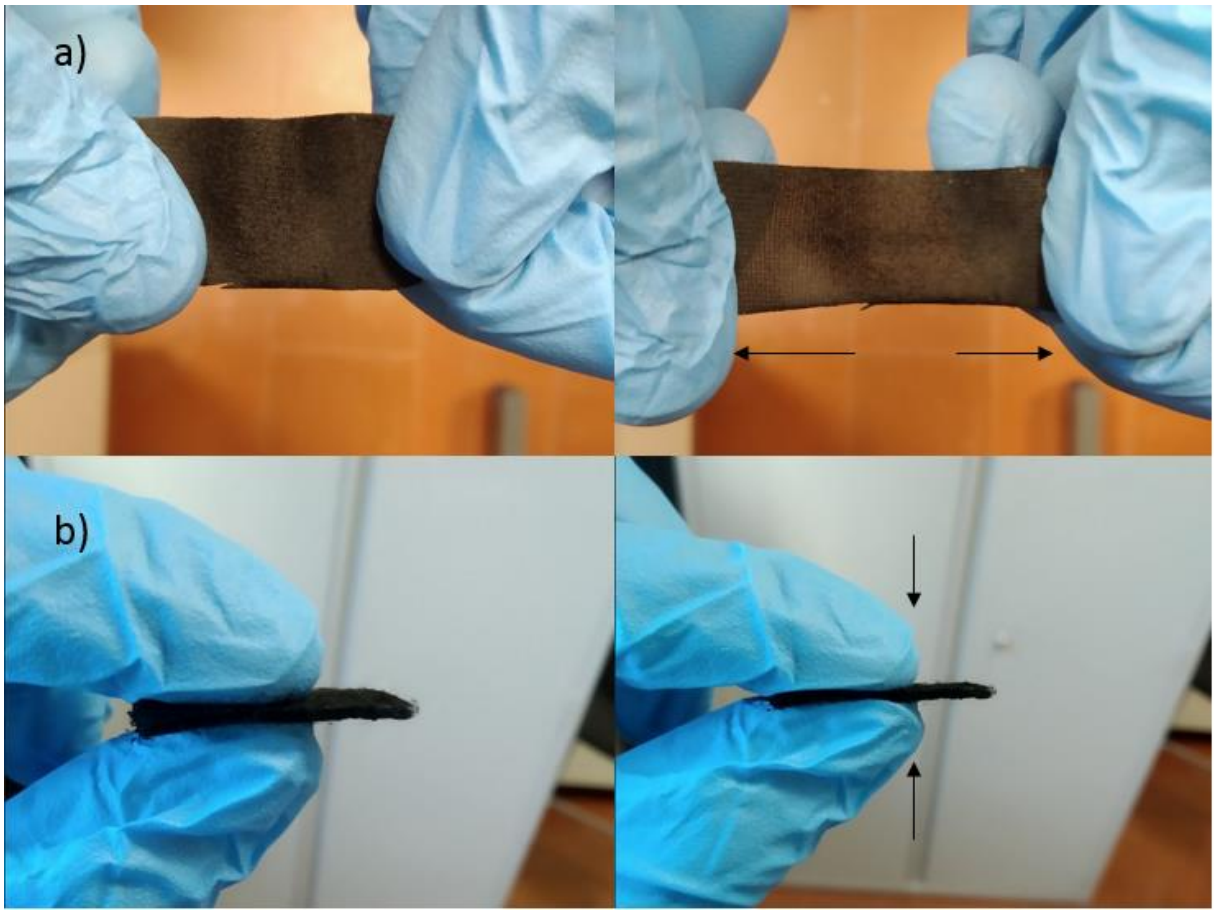

Figure 2.1-Visual representation of the applied forces to textiles. a) stretch on lycra textiles and b) pressure on felt textiles.

3 Results and Discussion

This section is dedicated to the characterization and detailed explanation of the conductive textiles. Starting from conductivities, morphology, piezoresistive behaviour and finally stability tests, this work intends to show a study of e-textiles, when intrinsically conductive polymers are used.

3.1 Textile characterization

Two commercial textiles were morphologically and chemically analysed: lycra and felt. Figure 3.1 shows macro- and microscopic morphology of fabric to understand the orientation of fibres for each textile.

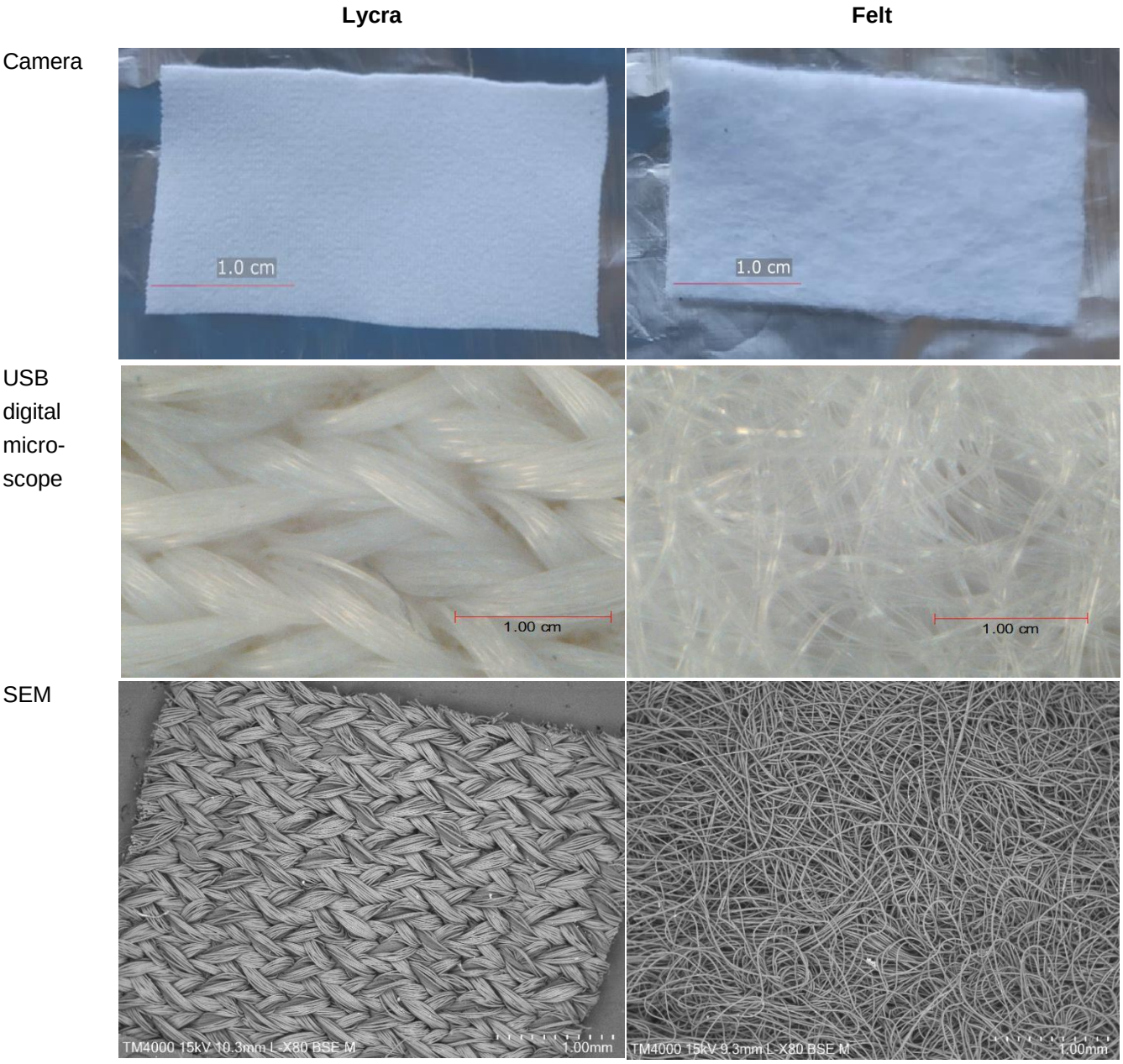

Figure 3.1-Macro- and microscopic morphology of lycra and felt textiles.

As previously mentioned in the introduction, lycra is a highly stretchable textile composed by fibres weaved with a unidirectional (course) preference, while felt is a nonwoven textile composed by randomly orientated fibres. Figure 3.1 shows the macroscopic image of both textiles as well as the microscopic images and analysis of fibres morphology that composed them.

For lycra, represented on the left, it´s barely possible to discern any fibre orientation on the macroscopic scale (arrow direction). But when seen with a microscope, it´s possible to see a course fibre orientation and how these fibres are interwoven. This direction, going from left to right, is named after courses (horizontal knitted rows), as it is the same direction that is used when mechanical stress is applied, when it is used in stretching tests.

On the right, it´s possible to see a macroscopic overview of felt-based textile. Its fibres are randomly organized. It has a cotton-like feel, but there is no preferential direction. For that reason, this textile was selected for pressure tests, as stress is applied through its thickness direction (wales).

The textiles were characterized for their physical properties before polymerization. In Table 3.1, weight, dimensions, thicknesses, resistivities, and maximum strain values are described. Strain is the physical deformation measured in percentage when stress is applied. In lycra´s case, this means the variation in length, Ɛ, described in formula 2. For felt, strain is the variation of thickness, also represented by Ɛ in formula 1.

Table 3.1- Textiles physical properties before polymerization.

	Dimensions (cm^2)	**Weight (g)**	**Thickness (mm)**	**Strain (%)**	**Electrical resistivity ($\Omega.cm^{-1}$)**
Lycra	6 (3x2)	0.120	0.33±0.01	65	$1.0x10^{13}$
Felt	6 (3x2)	0.128	1.17±0.01	30	$7.5x10^{7}$

As seen in Table 3.1, strains and thicknesses are very different for each textile, allowing for different sensing applications. It´s also important to notice that the value presented for lycra´s strain is applied to the main course direction, going from 35% in width to 65% strain in length direction.

3.2 Electrical characterization

Conductivity was studied, determining the best samples that were used for further tests, based on polymerization time, annealing temperatures and times, as seen in Table 3.2, for PPy samples.

Table 3.2- PPy synthesis parameters

Polymerization time (min)	**Annealing time (h), at**		
	Ambient temperature (25° C)	**60° C**	
30	Until dry	24	48
60	Until dry	24	48
120	Until dry	24	48
180	Until dry	24	48

The purpose of these parameters was to study how much did the synthesis polymerization time affected the conductivity, as seen in other works, higher polymerization times generated a darker black colour in textiles, where conductivity was higher, and resistivity values were lower, when compared to polymerization times of around 15~30 minutes, where the colour of the polymerized textiles was predominantly grey, conductivity values were lower, and resistivity values higher. The purpose of annealing times was to determine whether temperature would help stabilize the bonds of PPy-fibres and generate higher conductivities [3], [6], [14], [16], [21]. All tests were done with three samples per parameter, three times, averaging nine results.

To understand and quantify the electrical resistance change in a sample, on an order of a few cms, the following formula (1) is presented:

$$R = \rho \frac{l}{A} \tag{2}$$

Where R is the electrical resistance, ρ is the resistivity, l is the length of the sample that is being measured and A is the area of the sample [30][24]. Since we are working with a textile sample it´s important to denote that this formula applied to bulk area and volumes, not isolated fibres. Besides electrical resistance, that will be measured both in relaxed and stretched/pressed samples, depending on the sample being lycra or felt.

Two ways were conducted to measure conductivity: transversal and planar. The first measures conductivity through the thickness of the sample, while the second measures conductivity on the surface. To help better understand how conductivity is calculated, formula (2) is necessary. As seen, resistance can be calculated through resistivity and the area of the sample. A simple I-V curve is calculated with the help of a digital multimeter, and the slope of the linear function, representing the resistance, is used for the calculus. Electrical conductivity (σ) is described as the inverse of the electrical resistivity, given in $\mathrm{S.cm^{-1}}$, therefore:

$$\sigma = \frac{1}{\rho} = \frac{L}{R.A} \tag{3}$$

On equation (3), L/A, has different interpretations, being L the distance between electrodes, as represented in Figure 3.1. When transversal conductivity was studied, L was the thickness of the textile, while A was the area that was being measured on the surface (represented by d, length of electrode, and, l width of the electrode). When planar studies were being performed, L was the distance between electrodes (presented in Appendix B), while A was the multiplication of the textile´s thickness (µm) and the length of the electrode. Equations (3.1) and (3.2) show the precise interpretations of both transversal and planar electrical conductivities, respectively.

$$\sigma = \frac{1}{\rho} = \frac{L}{R.A} = \frac{L}{R(l.d)} \tag{3.1}$$

$$\sigma = \frac{1}{\rho} = \frac{L}{R.A} = \frac{L}{R(\mu m.d)} \tag{3.2}$$

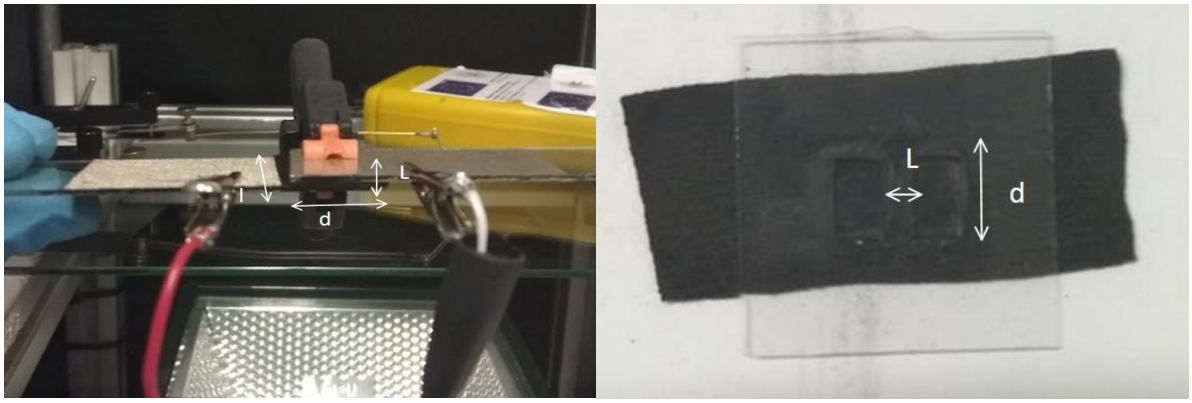

Figure 3.2- Visual representation of the dimensions used for conductivity tests. left- transversal; right-planar.

3.2.1 Polypyrrole conductivity

The first tests conducted were polypyrrole polymerized lycra, being the foremost concern understanding how the parameters presented in Table 3.2 influenced the conductivity results. The results are as described on Figure 3.3.

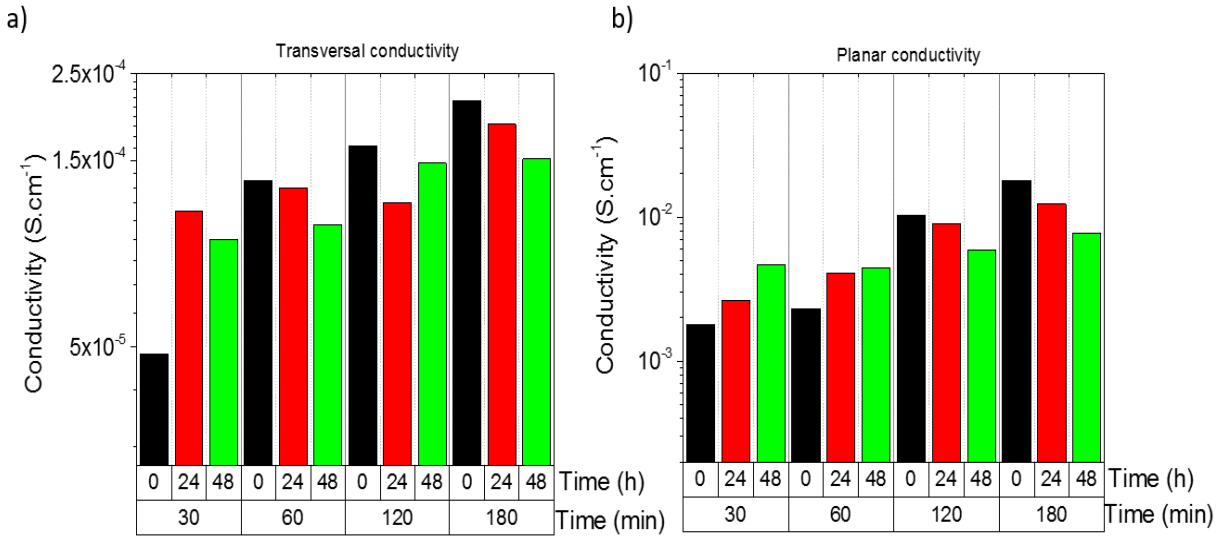

Figure 3.3-Conductivities of lycra textiles polymerized with PPy, The y-class represents conductivity in $S.cm^{-1}$, while the x-class represent the times. On the bottom are represented the polymerization synthesis times in min, while on top are represented the annealing's´: 0 represents the sample drying at ambient temperature, while 24 and 48 are the hours spent in annealing at 60° C. a) transversal tests; b) planar tests.

From Figure 3.3 it was possible to conclude two important notes. Firstly, the polymerization time for *in situ* chemical synthesis is a major factor, as it directly influences conductivity values. The longer the polymerization, the higher the conductivity for lycra textiles, and visually there´s also the effect mentioned in the bibliography [15], [32], [33], thirty minutes polymerized textiles presented a dark grey colour, while two- and three-hours polymerized textiles presented a darker colour, predominantly black. Secondly, the annealing studies concluded that there is no need for any annealing, as it does not produce any beneficial effects on the study conducted in this thesis. Other bibliographies support this claim, as they state how lower temperatures in the order of -10° to 0° C [14], produce better and more consistent

results, on chemical synthesis with agitation*. It´s also important to notice that since not all magnets and flasks are of the same size, there is some error associated with the results. The best-found condition was for three hours, left drying at ambient temperature Table 3.3 describes the conductivities and resistivities of the best parameter tested.

Table 3.3- Optimal lycra-PPy conductivity and resistivity values.

Optimal time condition and temperature	**Conductivity ($S.cm^{-1}$)**		**Resistivity ($\Omega.cm^{-1}$)**	
3h at 25° C	**Transversal**	**Planar**	**Transversal**	**Planar**
	$(2.129\pm0.998)x10^{-4}$	$(1.805\pm0.412)x10^{-2}$	$(7.00\pm4.91)x10^{3}$	(58.302 ± 12.760)

Through Table 3.3, the relation between conductivity and resistivity can be understood. From this relation it´s possible to see the lower resistivity values on the surface of the sample compared through its thickness. This happens, because the coating covers the surface much quicker than its thickness.

Felt was tested next. In Figure 3.4 we can see the conductivity values disposed of in the same-way as the previous tests.

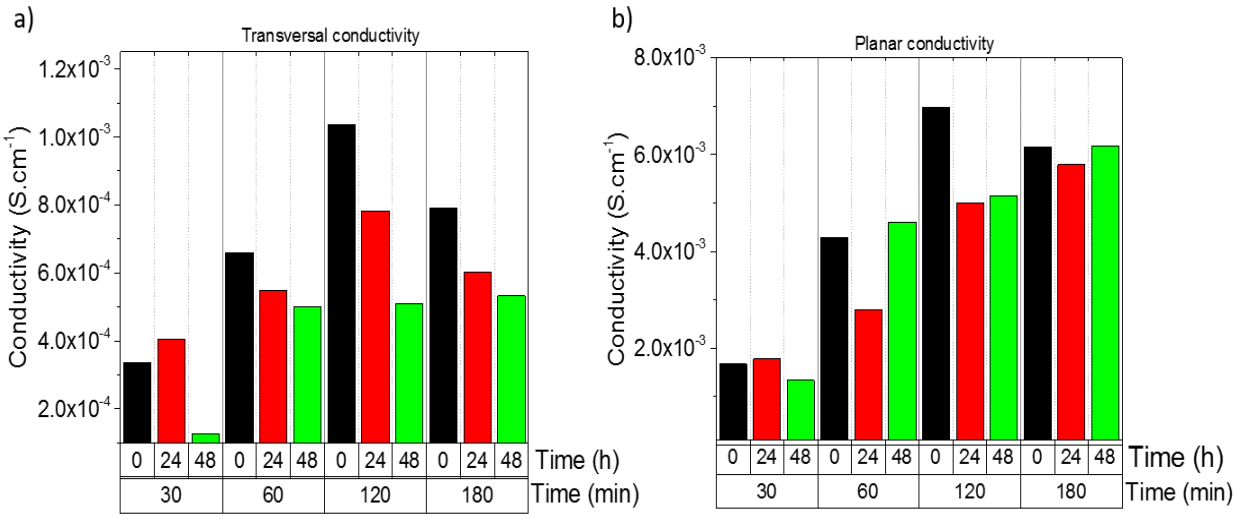

Figure 3.4-Conductivities of felt textiles polymerized with PPy, The y-axis represents conductivity in S.cm^(-1), while the x-axis represent the times. On the bottom are represented the polymerization synthesis times in min, while on top are represented the annealing's´: 0 represents the sample drying at ambient temperature, while 24 and 48 are the hours spent in annealing at 60˚ C. a) transversal tests; b) planar tests.

Felt was different from lycra as a textile for polypyrrole polymerization. For once, it was demonstrated that two hours showed better results than three. This might be because clusters of PPy are formed if polymerization is kept for a long time, being unable to conduct differences in electrical resistance as well. Since felt is more absorbent and has more randomly orientated fibres, it´s possible it doesn´t take as long for this effect to happen on felt compared with lycra. The values in transversal conductivity are higher when compared to lycra, proving the predisposition of this textile for pressure applications. The best-found condition was for two hours, left drying at ambient temperature, as seen in Table 3.4.

Table 3.4 shows a closer relation between transversal and in-plane values when compared to lycra. This happens for two reasons. Firstly, because felt absorbs more water than lycra, the polymerization is more efficient, resulting in more mass of ICP through its thickness. Also, because fibres are randomly orientated when compared to lycra it might be harder for the coating to stick to the surface. Therefore, when electrical tests are conducted, electrons have a harder "path" to travel, decreasing it´s conductivity. This last explanation can be justified looking at both textiles planar conductivities, lycra has a value of 1.805E^{-2} S.cm^{-1}, while felt has a lower value of 6.980E^{-3} S.cm^{-1}.

Table 3.4-Optimal felt-PPy conductivity and resistivity values.

Optimal time condition and temperature	**Conductivity (S.cm^{-1})**		**Resistivity (Ω.cm^{-1})**	
	Transversal	**Planar**	**Transversal**	**Planar**
2h at 25° C	(1.036±0.128)x10^{-3}	(6.980±0.500)x10^{-3}	(9.793±1.126)x10^{2}	(1.440±0.106)x10^{2}

3.2.2 PEDOT conductivity

After the conductivity tests for polypyrrole made clear which parameters were optimal, the same procedure was done for PEDOT. Since the synthesis was different, it was expected that the EDOT vapour used to polymerize the textiles would not come out so easily as PPy that created residues. The method used, soaking the fabric in an oxidant solution and then polymerizing at temperatures between 80° to 100° C was expected to achieve more uniform coating, resulting in a thin conducting polymer layer on the textile substrate [24]. No annealing times were studied, as the textile already spends a controlled amount of time in an oven. Figure 3.5 represents the conductivity values, studied by four different times: 30, 10, 180 and 300 minutes, three samples were used per time, and tested thrice.

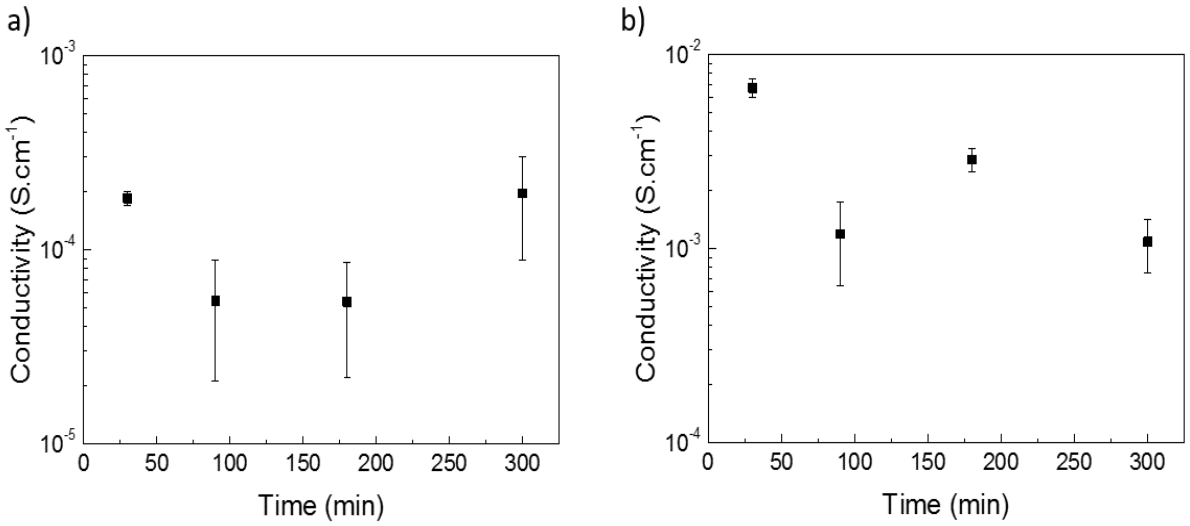

Figure 3.5-Conductivities of lycra textiles polymerized with PEDOT. The y-axis represents conductivity in S.cm^{-1}, while the x-axis represents the times in minutes. a) transversal tests; b) planar tests.

Table 3.5-Optimal lycra-PEDOT conductivity and resistivity values.

Optimal time condition and temperature	Conductivity ($S.cm^{-1}$)		Resistivity ($\Omega.cm^{-1}$)	
	Transversal	**Planar**	**Transversal**	**Planar**
30 min at 80℃	$(1.837\pm0.146)x10^{-4}$	$(6.707\pm0.737)x10^{-3}$	$(5.479\pm0.460)x10^{3}$	$(1.539\pm0.207)x10^{2}$

Because PEDOT is polymerized via chemical vapour deposition, the conductivity on the surface area should be more consistent than over its thickness. Nevertheless, not much error seems to be found in overall conductivities, spanning over an order of magnitude in both graphs of Figure 3.5. PEDOT seems to adhere to the fibres´ surface, meaning less time was required when compared to polypyrrole polymerizations. Since time did not seem to be a parameter of interest, as no linear correlation was found between higher times of synthesis and higher conductivities, it was decided to use the most economic parameter, both in time of synthesis and in amount of reagent used. All the tests that are further presented on this thesis used 30 minutes as the time of synthesis and a cooling of 15 minutes, before opening the flask, since temperature inside the oven is kept at 80° C. Also, the polymerization of EDOT into PEDOT through this method releases toxic vapours, requiring a more careful use. Table 3.5 describes the overall conditions of the most economic time.

Figure 3.6 represents the conductivities of felt textiles polymerized with PEDOT for both transversal and in plane conductivity configurations.

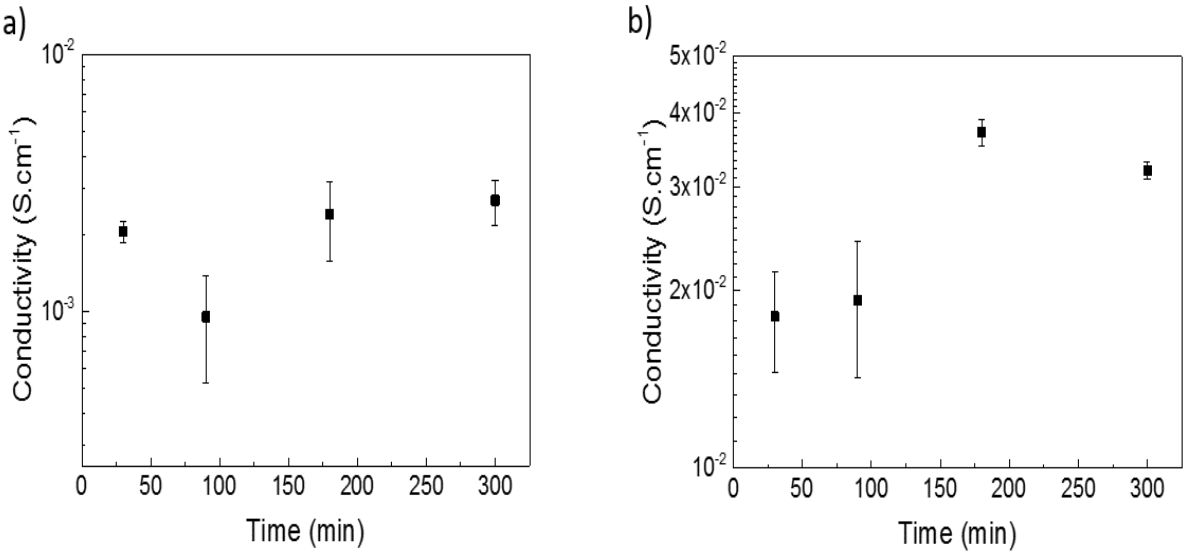

Figure 3.6 -Conductivities of felt textiles polymerized with PEDOT. The y-axis represents conductivity in $S.cm^{-1}$, while the x-axis represents the times in minutes. a) transversal tests; b) planar tests.

Felt´s conductivities reach the highest overall values on any textile studied in this work. In Figure 3.6 it's possible to see how most of the samples show almost no error associated, noticing that the position in which textiles are fixed during polymerization are not controlled. Like lycra, felt does not seem to present a fixed correlation between conductivity and time, since only one result diverges over one

order of magnitude from the rest of the samples. Despite the unevenness of felt´s fibres, conductivity values are very stable, more so than its counterpart, polypyrrole. Table 3.6 describes the overall conditions of the most economic time.

Table 3.6-Optimal felt-PEDOT conductivity and resistivity values.

Optimal time condition and temperature	**Conductivity ($S.cm^{-1}$)**		**Resistivity ($\Omega.cm^{-1}$)**	
	Transversal	**Planar**	**Transversal**	**Planar**
30 min at 80° C	$(2.040\pm0.190)x10^{-3}$	$(1.808\pm0.351)x10^{-2}$	$(4.936\pm4.32)x10^{2}$	(57.483 ± 11.154)

From the values present in Table 3.6 it is possible to consider surface conductivity as the best option for this textile, yet, since this work looks at the piezoresistive potential of fibres it is important to understand that the difference in conductivities happens in the relaxed state of samples. When stress is applied, electrical resistance ought to lower, significantly increasing conductivity in the thickness direction. Piezoresistive characterization studies this behaviour, for all textiles, using fatigue traction and pressure-strain tests.

3.3 Morphological characterization

3.3.1 SEM

Visual representation of the polymerized textiles under Scanning electron microscopy is quintessential to observe how the polymer coated the textiles. Figure 3.7 gives two different views of polymerized textiles, an overview of a section and a detailed view, where coating and aggregates of polymer can be seen.

All samples presented in SEM are taken from optimal polymerization parameters: 3 hours for lycra-PPy, 2 hours for felt-PPy and 30 minutes for both PEDOT polymerized textiles.

It´s possible to see the distribution of conductive polymers. Figure 3.7 shows how textiles are coated without fails, as each fibre presents coating of ICP, not discernible since particles could be in the size of nanometres and a more potent SEM would be needed to reveal the uniformity of these.

Fibre orientation show how polymer can aggregate. In case of lycra, because the fibres are interwoven and have more space between their course direction, the clusters tend to cluster more in that area, while felt textiles, show random disposition of fibre orientation, and as such, have random disposition of clusters, whether PPy or PEDOT which seem to adhere better to fibres on the surface with smaller spaces between them. The presence of densely packed micron-sized clusters are not desirable for fibre strain applications, as these generate more contacts in relaxed states of the textiles [24]. PEDOT prepared by chemical vapour shows a smoother surface on fibres when compared to a rougher surface seen on polypyrrole textiles, prepared by solution polymerization. Thinner coatings are beneficial in improving strain behaviour. Smoother and denser layers of ICPs are more resistant to chemical degradation due to fewer reactions with oxygen and water molecules, enhancing its stability [14]. An EDS morphological study, was conducted, showing the distribution of chemical elements along the surface of the textile (Appendix B, highlighting the high presence of N atoms in PPy samples and S atoms in PEDOT samples).

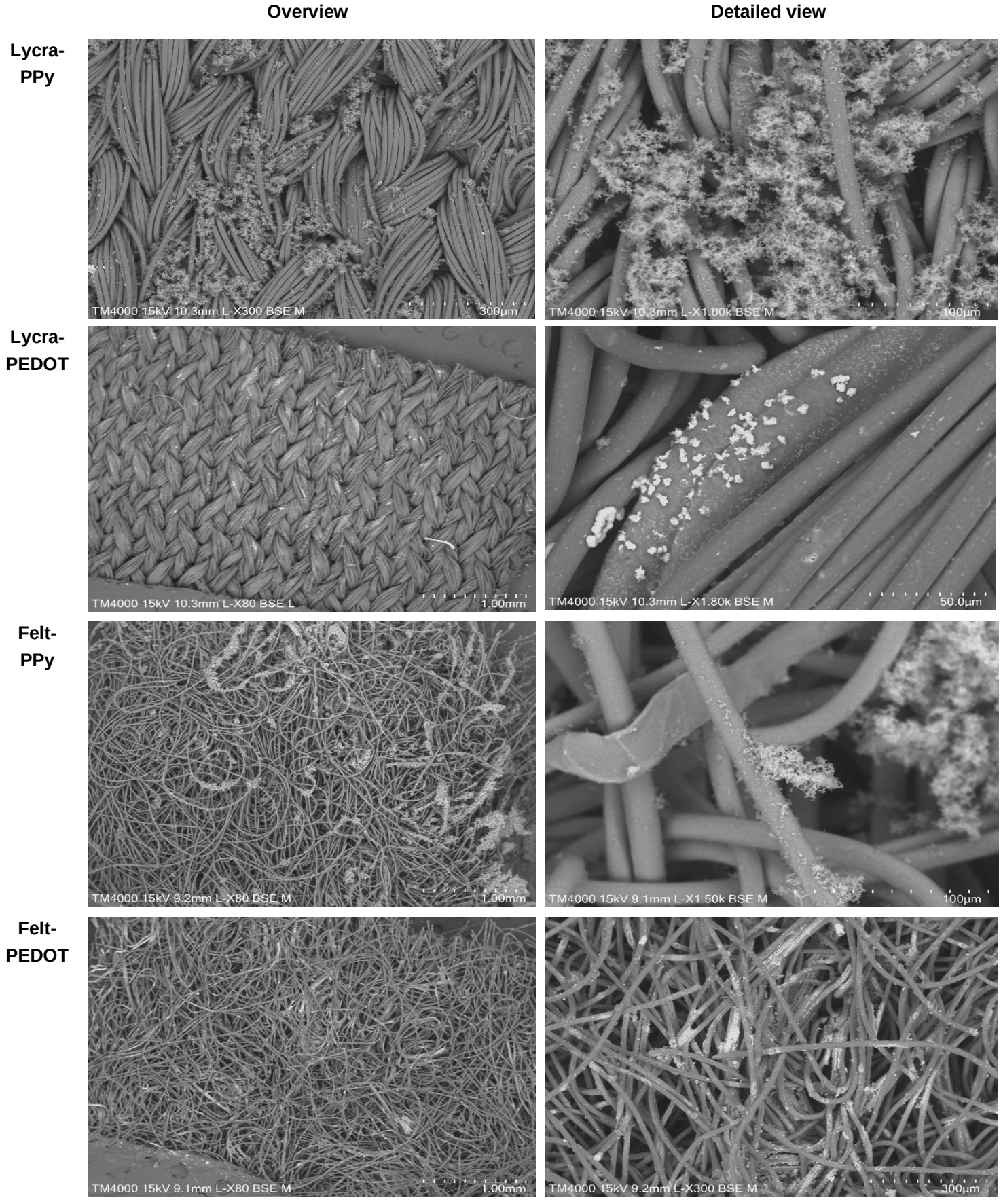

Figure 3.7-SEM images of polymerized textiles.

3.3.2 Raman spectroscopy

Raman tests were conducted to determine the chemical composition present in the textiles. The peaks seen in Figure 3.8 and Figure 3.9 represent chemical bonds. A laser with a wavelength of λ=533 nm and a power of 1 mW was used for the identification of specific bonds presented in the chemical structure on textiles.

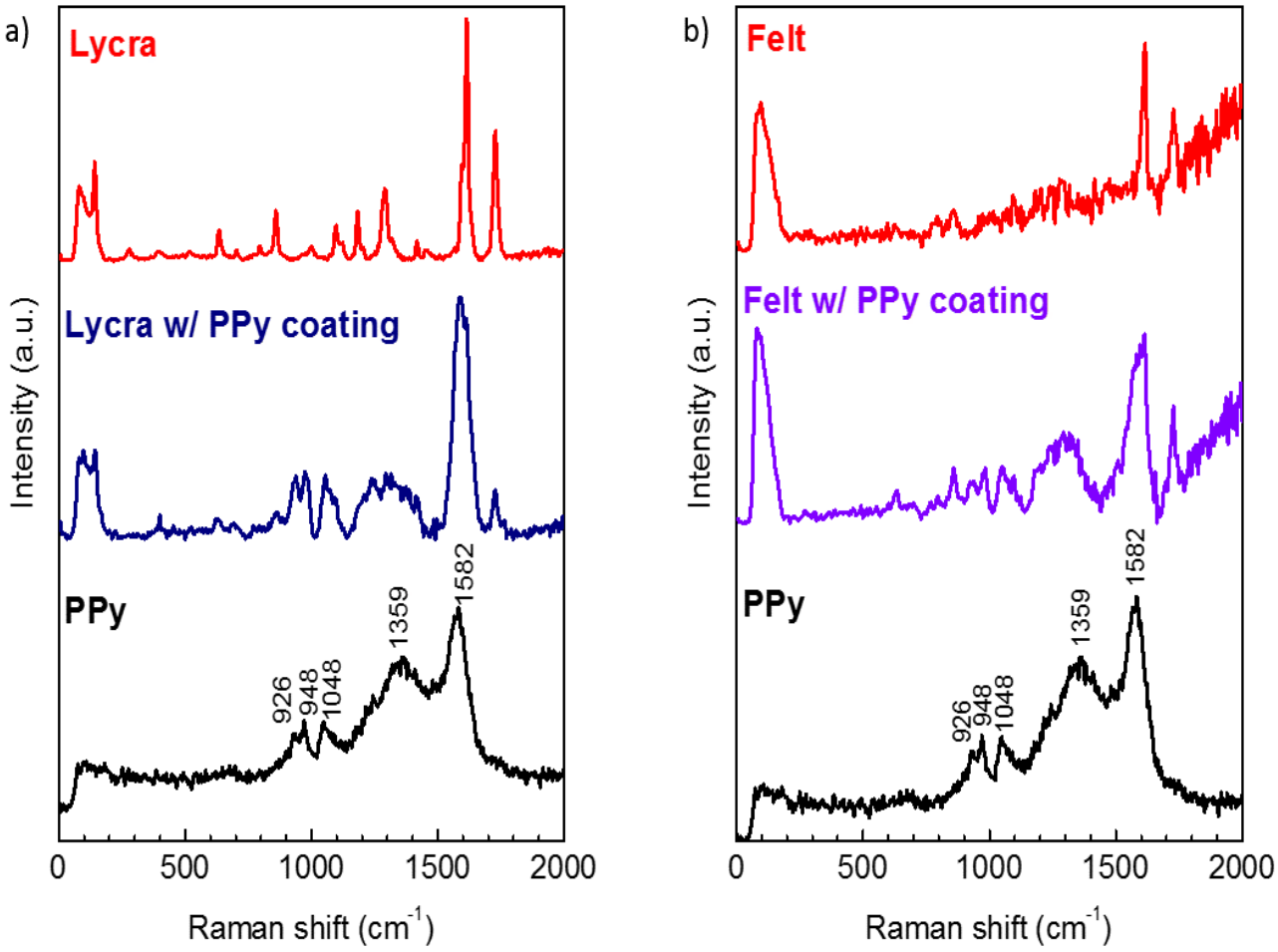

Figure 3.8-Raman spectroscopy of PPy polymerized samples: a) Lycra; b) felt.

and Table *3.8* explain the bonds in detail.

Figure 3.8 describes the chemical species present in polypyrrole textiles. Each graph represents 3 different spectra: textile, polymerized textile and material for comparison (PPy or PEDOT). It´s possible to see peaks in the polymerized textile that belong both to textile and to polymer, further confirming the presence of polymer.

The highlighted peaks are identified and described in

Table 3.7. The height of the peaks represents the relative concentration present, and width the structural disorder of crystallinity. Width of peaks is heightened in PPy due to its characteristic as an amorphous material.

All samples seen in Raman spectroscopy are from optimal polymerization parameters, that is 3 hours for lycra and 2 hours for Felt.

While it is not possible to see all peaks, such as out of plane deformation of C-H bonds, ring deformation or the N-H bond deformation that usually appears at 1260-1270 cm^{-1}, the most important ones are identified, especially the C=C bond stretching, along with the entire chain, and the slope present in 1600-1700 cm^{-1}, representative of the redox state of polypyrrole, while the slope is synonymous with the oxidation of PPy [8].

Table 3.7-Band assignments for Raman spectra of PPy at λ=533 nm

Raman shift (cm^{-1})	Description
926	Bipolaron species
948	Polaron species
1048	C–H in-plane deformation
1359	Ring stretching
1582	C=C backbone stretching

Figure 3.9 describes the Raman spectra of PEDOT samples, using the chemical peak identification of PEDOT: PSS. Since only PEDOT was used in polymerization, the peaks that represent PSS, which are identified in Table *3.8* do not translate to PEDOT polymerized textiles. The textiles used were polymerized using the most economic polymerization parameter, that is 30 minutes.

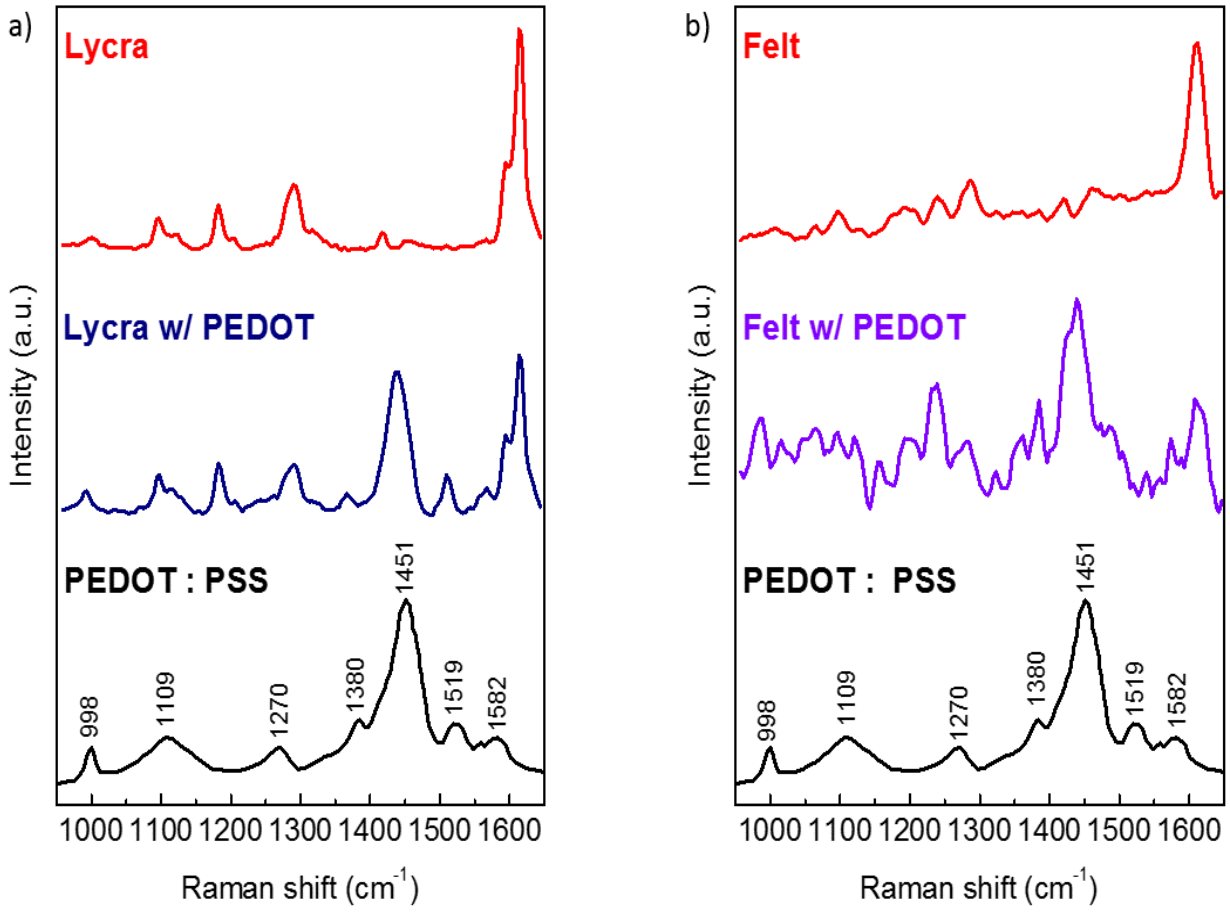

Figure 3.9--Raman spectroscopy of PEDOT polymerized samples. a) Lycra; b) felt.

Table 3.8-Band assignments for Raman spectra of PEDOT at λ=533 nm.

Raman shift (cm^{-1})	Description
998, 1109, 1582	PSS
1270	$C_\alpha - C_{\alpha'}$ inter-ring stretching vibrations
1380	$C_\beta - C_\beta$ stretching
1451	$C_\alpha = C_\beta$ symmetrical
1519	$C_\alpha = C_\beta$ asymmetrical

Besides the peaks described in Table 3.8, there is a Raman shift from 1272-1383 cm^{-1}, indicating a reduction in the intensity so that the $C_\alpha - C_{\alpha'}$ and $C_\beta - C_\beta$ changes to $C_\alpha = C_{\alpha'}$ and $C_\beta = C_\beta$. Therefore, the conformation of the PEDOT changes from a benzoid structure (coil conformation) to a quinoid structure (linear conformation) [6], [21].

As previously stated, Raman characterization did confirm the presence of ICP in textiles, as expected.

3.4 Piezoresistive characterization

3.4.1 Fatigue traction tests

Fatigue traction tests were conducted on lycra textiles in order to study the influence of mechanical stress on electrical resistance. Optimal conditions of three hours polymerization times for PPy and thirty minutes for PEDOT are studied in detail. Figure 3.10 shows the assembly that was used to get a uniaxial controlled strain of 5mm on textiles.

The main components that were used to control the tests were an Arduino (1), which was connected to a computer while running a specific code, a stepper driver (2), which had the connections between inputs and outputs of the Arduino to control and measure the stepper motor (3), which had the function of turning a co-axial controlled rotation into an unidirectional path where the support and textile (4) were fixed. Lastly a power supply (5) was used to feed the stepper driver (the schematic and code can be seen in Appendix C).

Working range, the difference between the resistance in the relaxed state and when strained and gauge factor (sensitivity) of the textiles was evaluated, while hysteresis, linearity and LOD (limit of detection), which is the minimum stress required to see change in electrical resistance values were not possible to determine due to the machine inefficiency to carry out stretching without limitations. On Table 3.9 a list of samples and their characteristics are described.

Fatigue tests were done with an extension of 5mm, resulting in a strain of around 17%. It is expected better results in sensitivities with higher strain (Table *1.1*). This limitation was due to the need of having no sliding of the sample when an unidirectional stress is applied, resulting in forces in the vertical direction of fibres (wales).

While conductivity of these textiles shows interesting values for this technology, maintenance of sensors remains a challenge, as room temperature prepared textiles see conductivity declines from reacting with atmosphere gases. Investigation has been conducted, describing declines up to ~80% of initial conductivity values, incentivizing low temperature polymerization, below -10 °C [14].

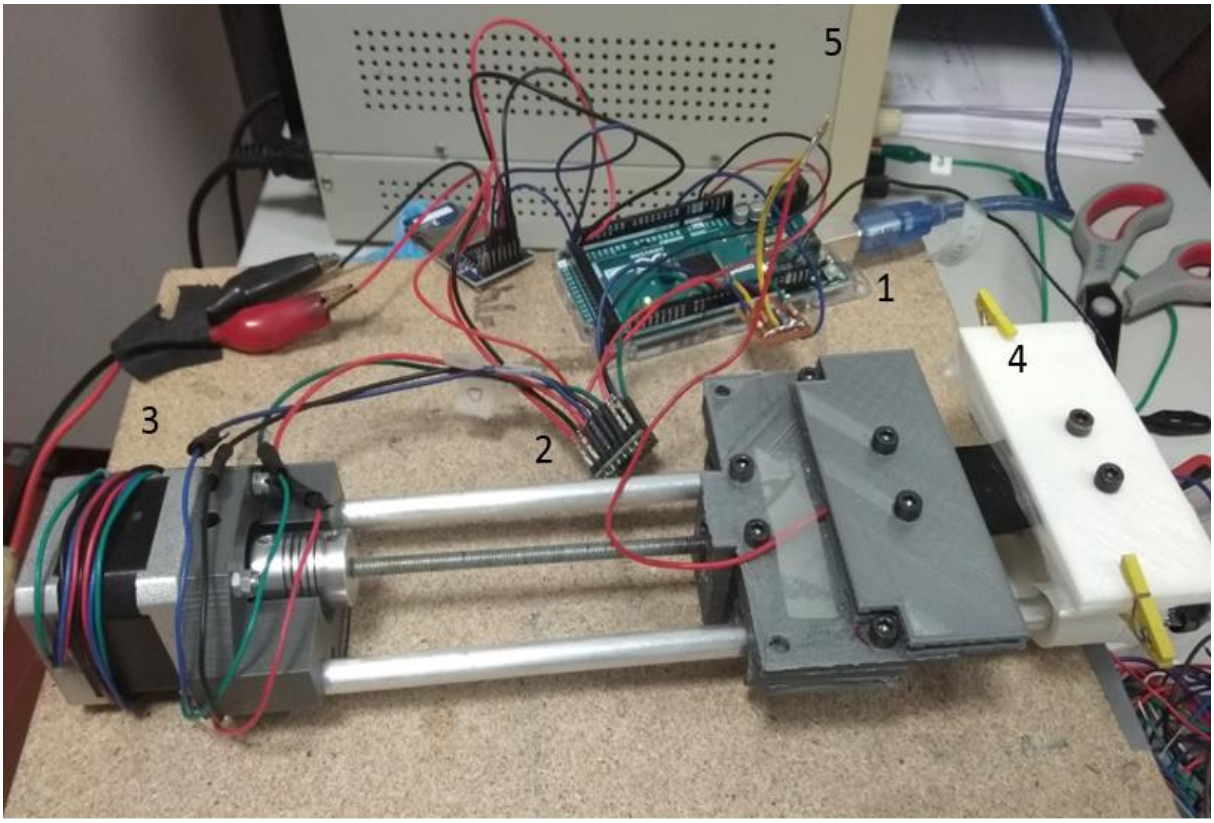

Figure 3.10-Assembly of stretch-strain test machine.

After assembly, two types of cycles were conducted: a 10-cycle test to understand reversibility of the electrical resistance behaviour and determining gauge factor, and a 300-cycle test to understand how fatigue changed the behaviour of the textile when exposed over a long exposure of stress. Figure 3.11 shows both tests for a lycra-PPy textile, while Figure 3.12 shows both tests for a lycra-PEDOT textile.

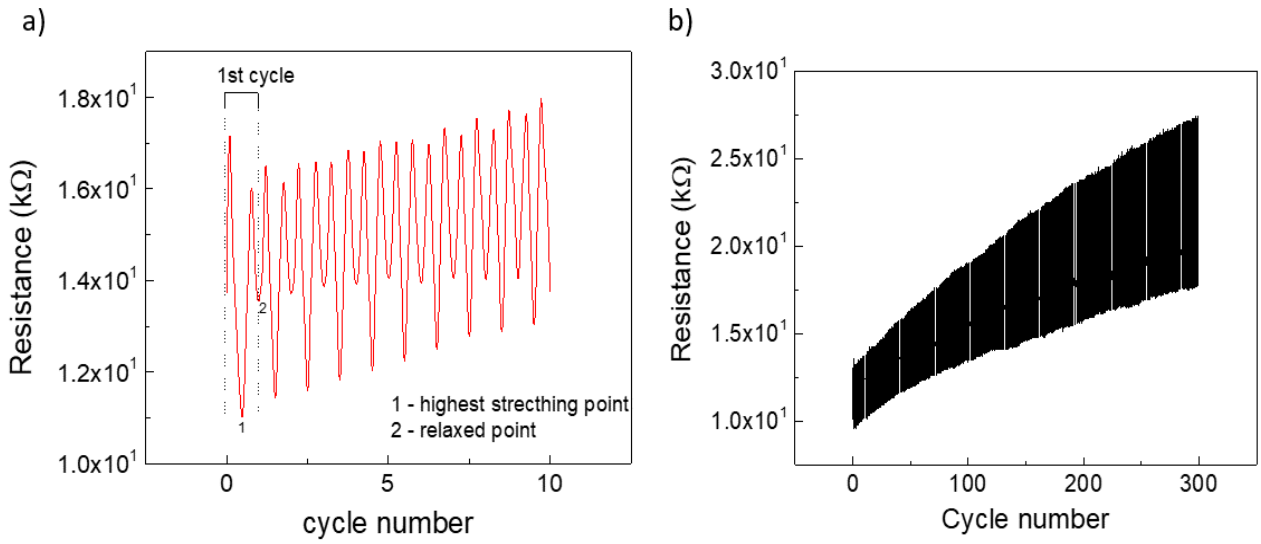

Figure 3.11-Stretch tests on lycra-PPy textiles. a) 10 cycles; b) 300 cycles.

The behaviour of the samples to fatigue tests is not linear. At first, the resistance increases with strain, and only then does the electrical resistance declines. The resistance of polypyrrole coated textile changes significantly at low strains due to the improvement of alignment of the polypyrrole chains and fibres within the coated fabric. When continuing to stretch the fabric to a large strain, it will reach the maximum degree of alignment of the polymer chains within the coated textile. The resistance of the PPy-coated lycra fabric will not change anymore [9], [13].

This behaviour of electrical resistance shifts when stretching or relaxing a textile as opposed to a linear increase or decrease of that measure was better described as following: as stretching increases, so does electrical resistance, since contacts become further apart, decreasing conductivity. But as that stretching develops into higher strains, the thickness of said textile also decreases, and so, the transversal conductivity of ICPs play a role in the results of an unidirectional stretch. When relaxation of the textile occurred, electrical resistance increased since transversally, there is relaxation as well before decreasing to a minimum, where strain is not applied.

It´s also possible to see different work range over 300 cycles, meaning the conductive polymer showed plastic behaviour, that is, deformation started to happen, cracking uniformity of the coating. This translates in higher electrical resistances, working range and gauge factor. While it might be a downside to have higher electrical resistances in piezoresistive applications, higher working ranges and gauge factor have the advantages of being able to measure higher ranges of motion. To effectively characterize this application as a sensor further tests about linearity and hysteresis should be conducted on a proper traction machine. Even though SEM wasn´t repeated after fatigue tests, coated materials textiles didn´t show fails in coating, unlike what is expected from films [3]. This further confirms the viability of ICPs in stretching sensors. Sensitivity values results are similar to what was expected, when compared to other works [13], [23], [24].

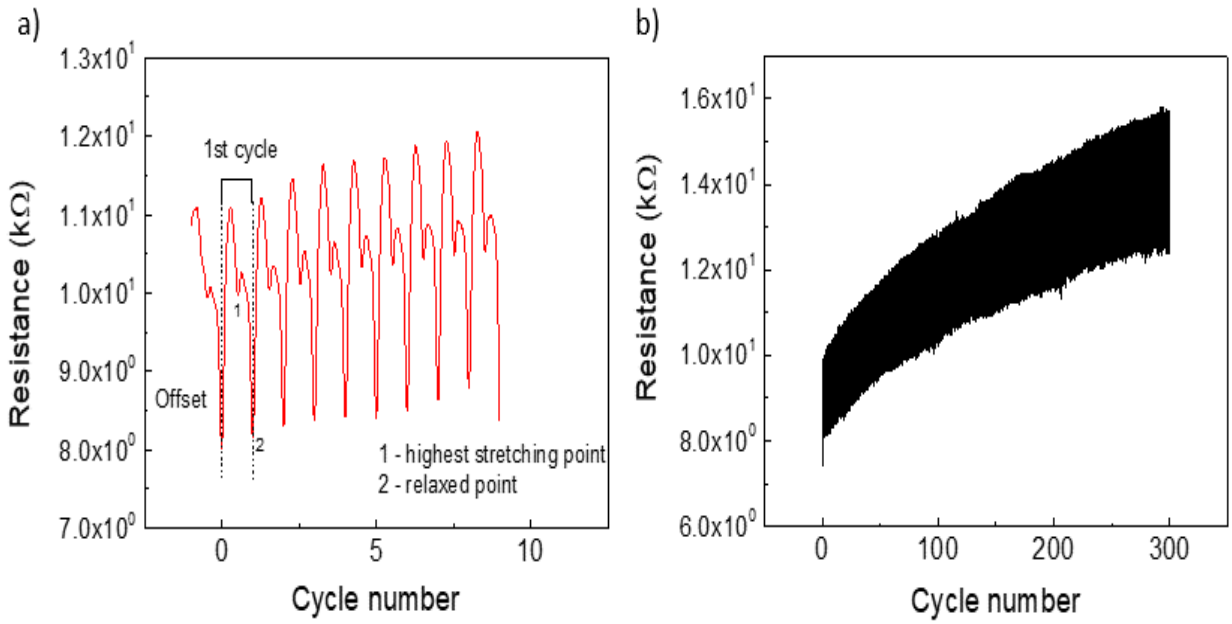

Figure 3.12-Stretch tests on lycra-PEDOT textiles. a) 10 cycles; b) 300 cycles.

Table 3.9-Fatigue traction test metrics.

Sample description	Number of cycles	Working range (kΩ)	Gauge factor
PPy-lycra	10	4.80 ±0.49	-2.10
PEDOT-lycra	10	3.11 ±0.14	-1.72
PPy-lycra	300	4.80 – 9.50	(-2.10) – (-2.90)
PEDOT-lycra	300	3.11 – 3.32	(-1.72) – (-1.61)

3.4.2 Pressure tests

Pressure-strain tests were then conducted on felt textiles. Optimal conditions of two hours polymerization times for PPy and thirty minutes for PEDOT are studied to detail. Figure 3.13 shows the assembly that was used.

The main components that were used to control the tests were an Arduino (1), which was connected to a computer while running a specific code, a voltage divider connected on a breadboard (2), which had the connections between inputs and outputs of the Arduino to measure resistance connected to conductive tape placed between the textile (3), and a support structure for measured weights (4), using the area of contact to calculate applied force (the schematic, code and design of the montage can be seen in Appendix D).

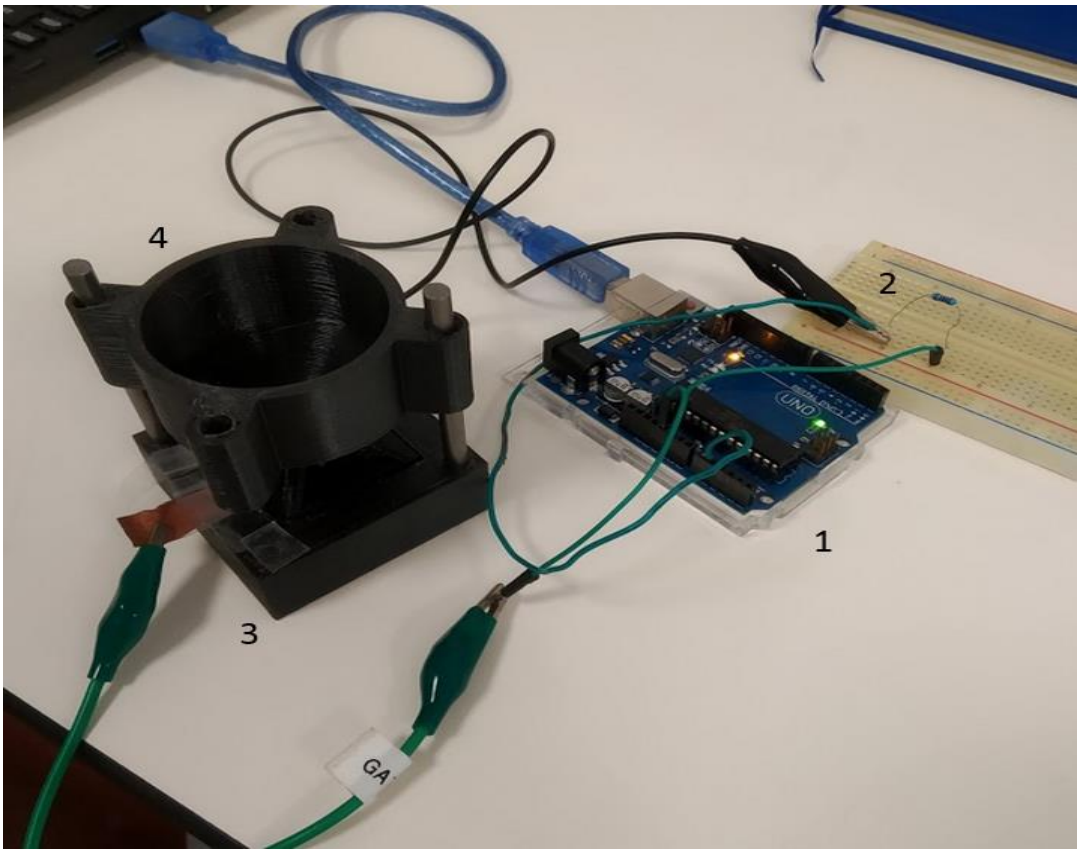

Figure 3.13-Assembly of pressure strain test machine.

Working range, gauge factor and linearity, the amount of time it takes the sensor to stabilize the value, were studied in pressure tests at different pressure regimes, low pressure (<10 kPa) and medium pressure (10-100 kPa) [34]. The values are presented in Table 3.10. It´s important to notice the initial values are incoherent, since the support structure isn´t applying any pressure, and therefore are not accounted in the sensor parameters. A filter (red data in graphs) was applied to the data, in order to reduce noise. The arrows represent the moment when weight was applied (black) or removed (orange).

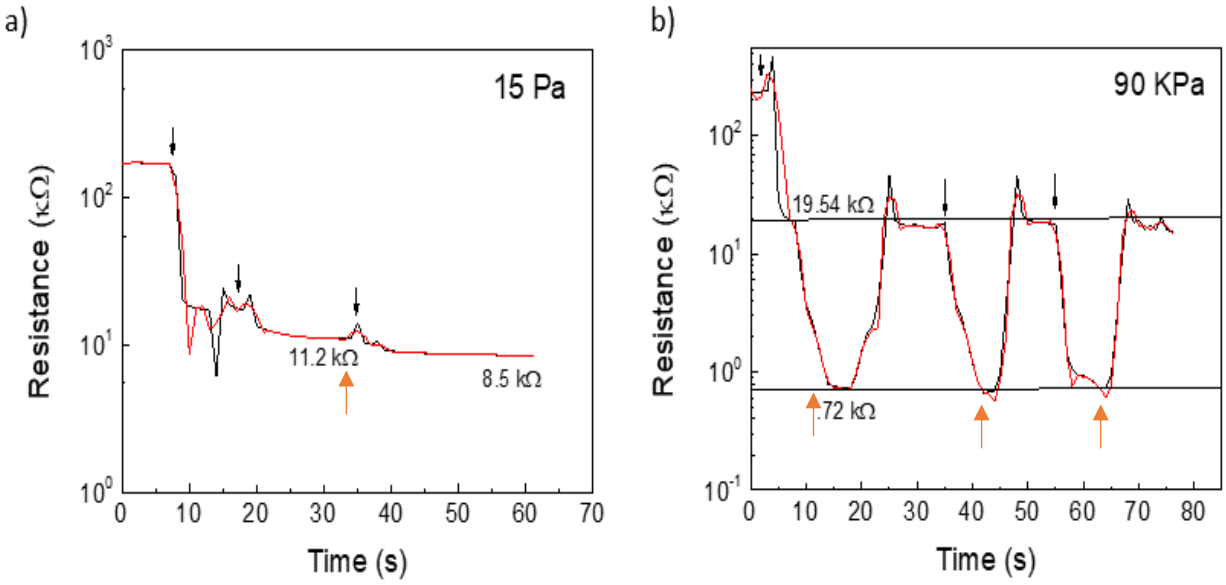

Figure 3.14-Felt-PPy pressure tests. a) low pressure; b) high pressure.

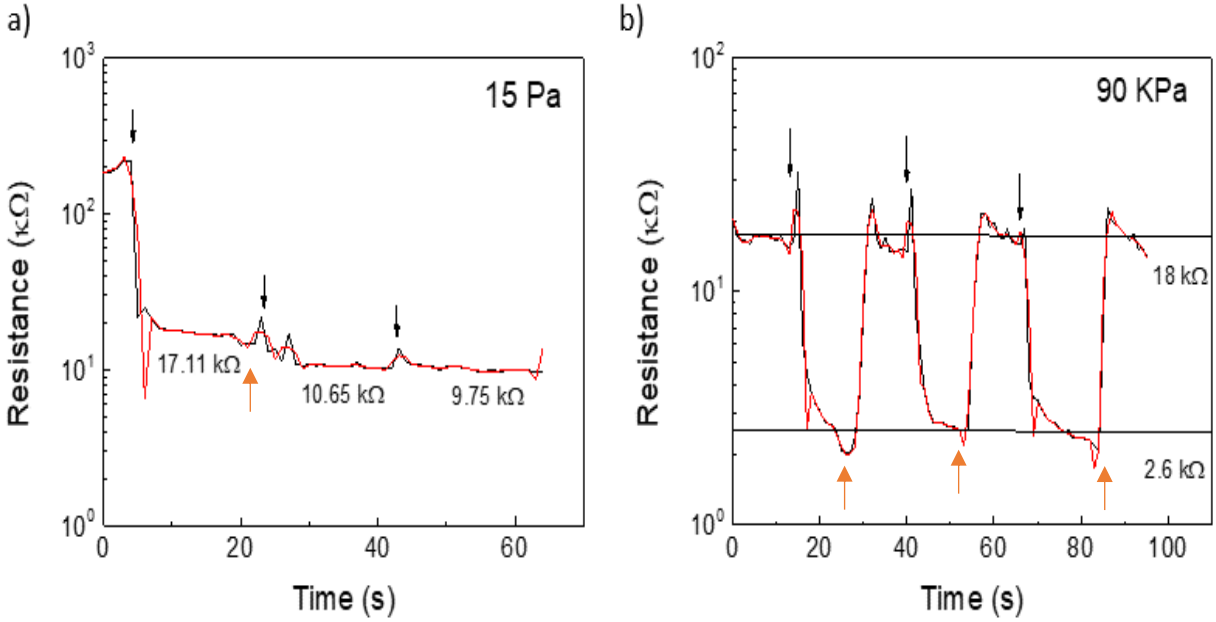

Figure 3.15-Felt-PEDOT pressure tests. a) low pressure; b) high pressure.

Table 3.10-Pressure tests metrics.

Sample description	Pressure regime (Pa)	Working range (kΩ)	Gauge factor	Linearity (s)
PPy-felt	Low (15)	9.152	1.55	12
PEDOT-felt	Low (15)	7.36	2.15	10
PPy-felt	High (90 k)	18.82	2.20	6
PEDOT-felt	High (90 k)	15.40	3.05	8

In Table 3.10 the working range and gauge factor both increase when higher pressure is applied, while linearity decreases. This can be explained because higher pressures lead to more applied strain, therefore the thickness of the textile lowers, and more conductive polymer comes into contact, meaning electrical resistance significantly decreases. Higher working ranges means the sensor can measure wider pressure values, while gauge factor is the sensibility of the sensor, meaning it´s more precise on higher pressure regimes, than for a lower regime of 15 Pa. Linearity decreases, further proving the sensor effectiveness in higher pressures, since it takes less time to stabilize the real resistance value [34][35].

3.5 Stability tests

This section´s purpose is to understand how these functionalized fibres hold on a regular day-to-day basis. Three tests were conducted: abrasion, conductivity over time, and washing cycles. Abrasion tests are meant to understand how friction between simulated skin and these textiles wears out over time. Conductivities over time are a monitorization of tests meant to understand if the parameters observed in conductivity characterization decays over time and how much, compared to the initial values. Washing cycles simulate a household washing machine, to understand if these textiles would have several uses as a commercial product.

3.5.1 Resistance to abrasion tests

For abrasion tests, a 3-D printed machine with controlled rotations over a certain frequency was used in order to serve as a substrate for the samples to perform several abrasion cycles. A support encased by pig skin weighted with leads performed a sweeping movement, creating friction between the simulated skin and the textile.

The frequency was controlled by an external power supply, and the tests took around five hours to complete totalling 10,200 cycles. Figure 3.16 shows a visual assessment of three samples, for each studied condition, each having three samples: before, abrasion, halfway through the tests (two hours and half, or 5,100 cycles) and after five hours.

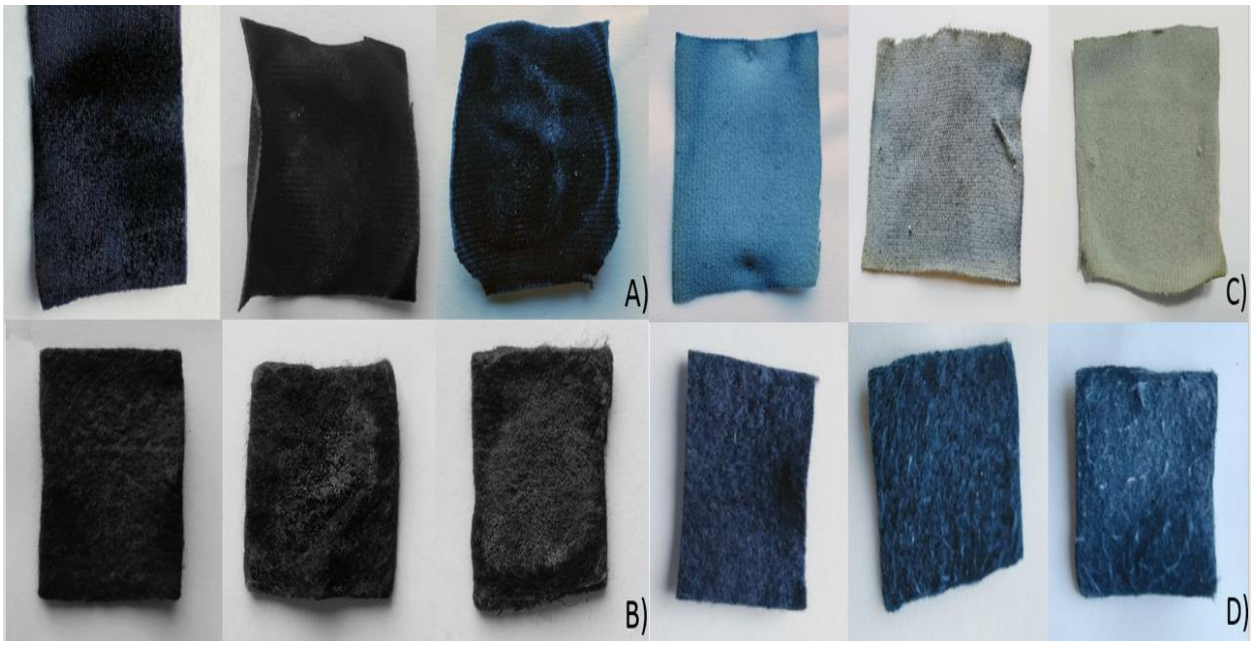

Figure 3.16-Visual representation of abraded textiles with controlled times:0, 2:30 and 5 hours. a) lycra-PPy; b) lycra-PEDOT; c) felt-PPy; d) felt-PEDOT.

As seen in Figure 3.16, the textiles were severally worn out. For lycra with PPy, A), a loss of colour can be seen. Although PPy polymerized textiles had polymer residues on their surface, the textile shows some white patches in the centre, where PPy was moderately abraded. While lycra with PEDOT, C), shows the worst visual evolution out of all tested samples. The blue colour characteristic in PEDOT, almost entirely dissipates, leaving the yellow colour from the oxidant more exposed. Comparing textiles B) and D), the same point can be made, as PPy felt samples have better polymer adhesion than PEDOT samples. While most of the loss of PPy in B) is due to the residues, the superficial fibres in D) are far more abraded, as some don´t even adhere any polymer. This effect is reported on other works [36]–[39], since solution polymerization method always gave a product with a better coating resistance, when compared to vapor polymerization method. This is attributed to the extended time that is required for the solution polymerization process. As the textile sample was left in water for 2-3 hours, the oxidant had sufficient time to fully penetrate into the wool strands, whereas vapor polymerization occurred much more rapidly and most coating was applied on the surface[39]. Methods for improvement of adhesion of ICP coatings have been studied, showing that atmospheric plasma treatments modify the surface energy of a textile, achieving surface modification while maintaining the bulk properties. Atmospheric plasma treatment generates different plasma constituents like electrons, ions, free radicals, meta-stables and UV photons. These either directly or indirectly participate in plasma-chemical reactions which introduce reactive groups and free radicals onto the surface, thus improving the adhesion of chemicals and polymers mostly by improved physical interaction[37], [39].

Because samples were fixed to a substrate using glue, both surface and chemical adhesion and bonds have lowered conductivity values more than just abrasion, since glue is an insulator. Figure 3.17 and Figure 3.18 show the decline in planar conductivity of the best-preserved textiles after tests.

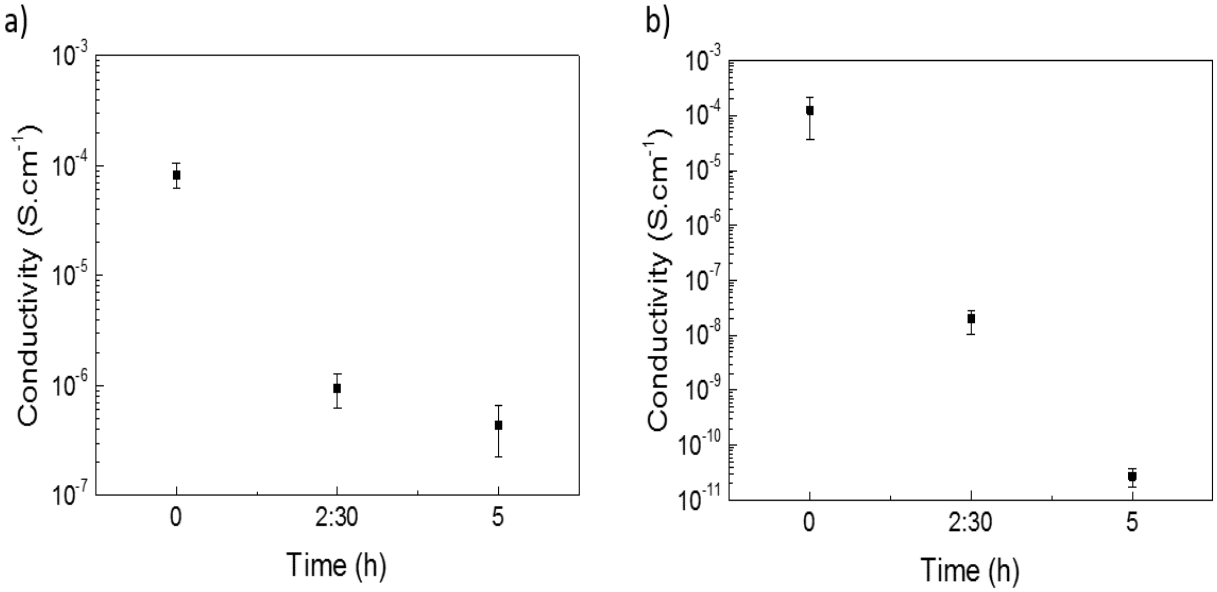

Figure 3.17- Planar conductivity of abraded lycra samples. a) PPy; b) PEDOT.

As seen in Figure 3.17, all lycra samples suffer a great decline, specially lycra-PEDOT, which visually is also seen as the textile in the worst condition after abrasion. Half-times of tests also show that textiles don´t hold too well even with half the cycles, since at half-time the conductivity values are already much lower, when compared to the initial conductivities.

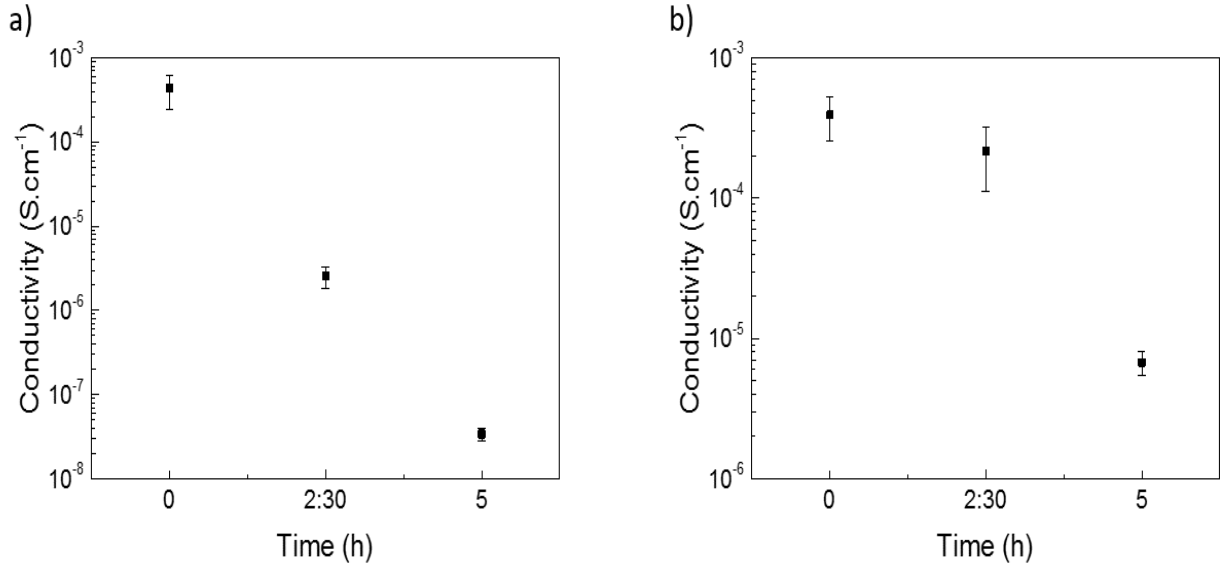

Figure 3.18-Planar conductivity of abraded felt samples. a) PPy; b) PEDOT.

Figure 3.18 shows how conductivity values change with abrasion. While similar to lycra in the fact that over 10,000 cycles the conditions worse drastically, it´s important to note that the same values aren´t as bad at half-time, especially on PEDOT, meaning felt samples have more longevity as a textile that is constantly abraded.

3.5.2 Washing cycles

The textiles were washed over 10 cycles, each for a duration of 30 minutes, using 100mL of H_2O and 0.2mL of commercial laundry detergent. The results are described in Figure 3.19 and Figure 3.20.

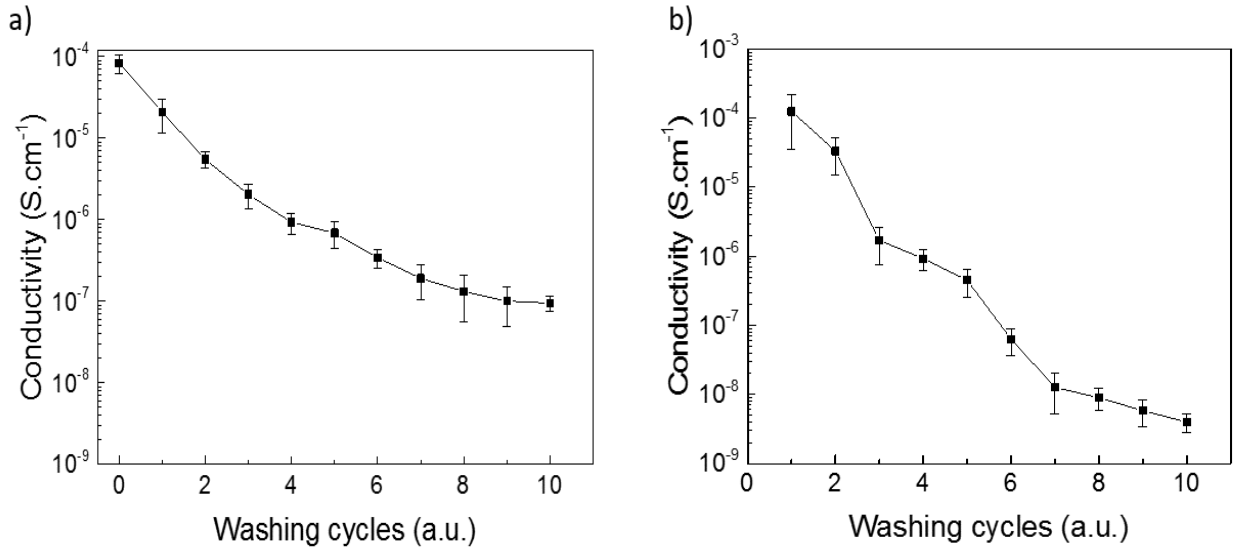

Figure 3.19- Transversal conductivity after washing cycles of lycra samples. a) PPy; b) PEDOT.

The lycra textiles suffered an almost linear decline in conductivity, showed in Figure 3.19 from their maximum measured value, $7.248^{-5}\mathrm{S.cm^{-1}}$ for polypyrrole and $1.255^{-4}\mathrm{S.cm^{-1}}$ for PEDOT, and their lowest measured value $9.505^{-8}\mathrm{S.cm^{-1}}$, for PPy and $1.023^{-9}\mathrm{S.cm^{-1}}$for PEDOT, after 10 washing cycles. This is because washing cycles are a way of abrasion in textiles, resulting in physical damage that may distort the fabric, cause fibres or yarns to be pulled out or remove fibre ends from the surface [36].

It´s thus understandable that lycra-PEDOT suffers such a decline in conductivity as chemical vapour deposition of the polymer affects coats superficial fibres more easily, and since lycra is a low thickness textile, abraded superficial fibres result in a loss of conductivity of almost 5 orders of magnitude.

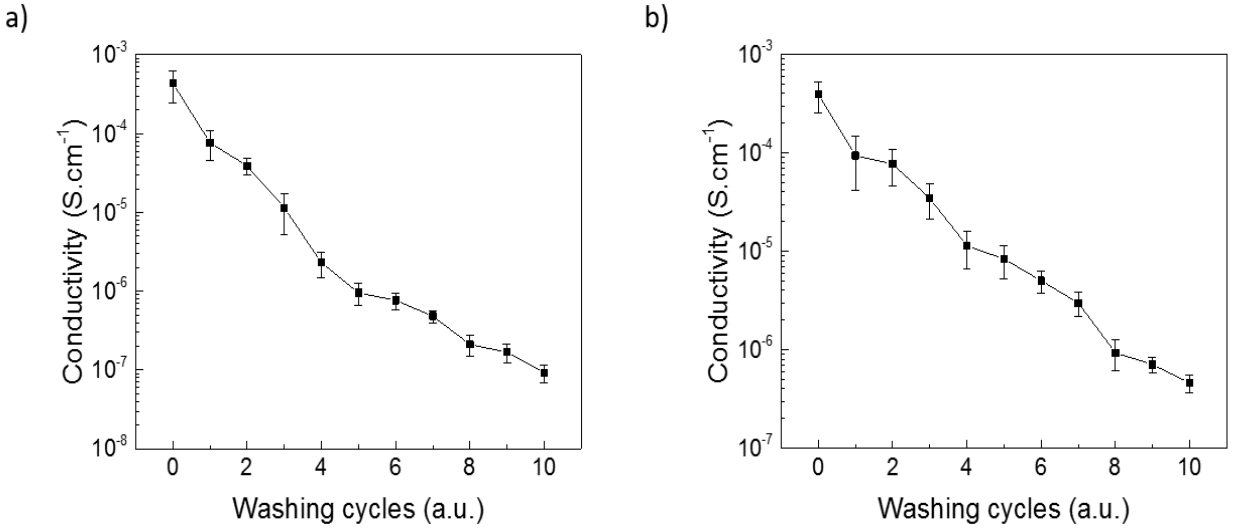

Figure 3.20- Transversal conductivity after washing cycles of felt samples. a) PPy; b) PEDOT.

Figure 3.20 shows the transversal conductivity decline suffered by felt textiles, when submitted to washing cycles.

The polymer's behaviour to the washing cycles showed a steady decline, from their maximum measured value $4.357^{-4}\mathrm{S.cm^{-1}}$, for polypyrrole and $3.914^{-4}\mathrm{S.cm^{-1}}$ for PEDOT, and their lowest measured value $9.123^{-8}\mathrm{S.cm^{-1}}$, for PPy and $4.574^{-7}\mathrm{S.cm^{-1}}$ for PEDOT, after 10 washing cycles.

Similar results have been reported in other works, showing how electrical conductivity declines and gauge factor values worsen with continuous washing. Other technologies, such as rGO/SWCNT coated fabrics show unchanged sensing response after 10 times of washing [24].

3.5.3 Conductivity over time

Conductivity over 6 months was studied to show the stability of samples. 2 samples of each textile were kept in storage, away from humidity and light, but in open air. Figure 3.21 describes the decline in conductivity for each textile polymerization.

Data is separated by colours: polypyrrole textiles are shown in black and PEDOT textiles are shown in blue for better differentiation. It´s possible to see how felt textiles are usually more stable and have overall higher conductivities when compared to lycra textiles counterparts. This is especially visible on PEDOT samples, and it puts the question of how polymerization times affect textiles. As felt needed less time for PPy polymerization, the same might be true for PEDOT, meaning more thickness and absorbance play a key role in stability for e-textiles.

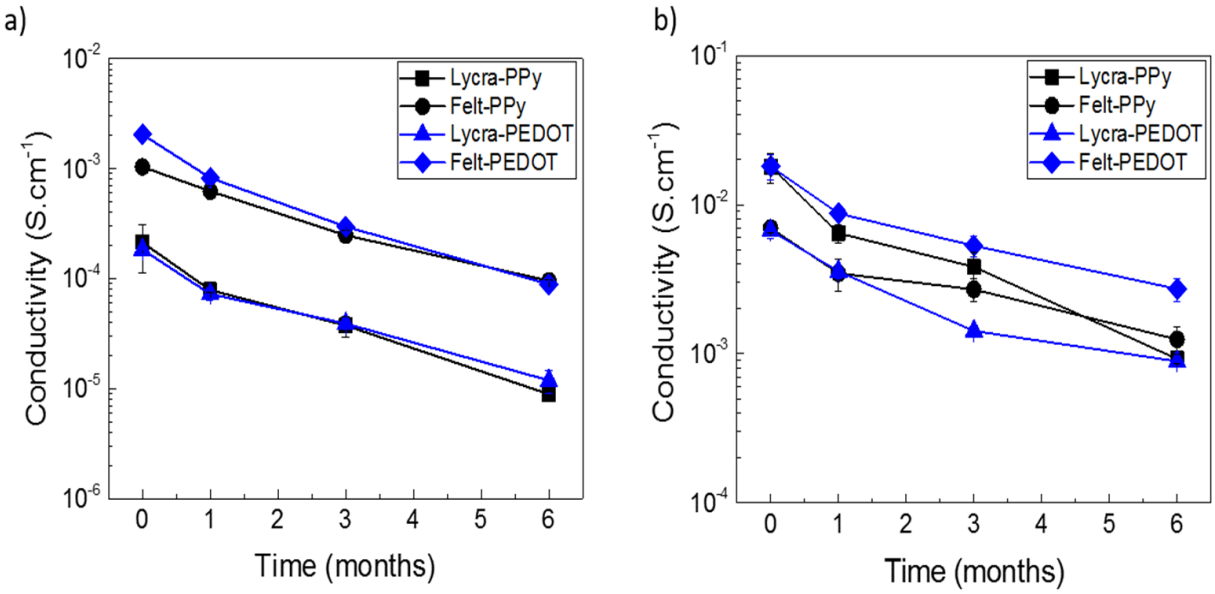

Figure 3.21-Visualization of conductivity decline over 6 months: a) transversal, b) in-plane

As it´s possible to see, while conductivities decrease over time, they do so in a stable, controlled way, and the impact is much less when compared to abrasion or washing tests. This decline happens because conducting polymers react with atmospheric chemicals, especially oxygen [9], [13].

To solve the challenge of conductivity loss, methods reported in literature such as use of specific dopants, surfactants, low-temperature polymerization, encapsulation or simply transferring conductive polymers to yarns instead of fibres is noted as a point of interest in future works [12], [14], [32], [36], [40].

Conclusion and Future Perspectives

The present work was focused on the production and characterization of e-textiles, to achieve stable functionalized commercial textiles with piezoresistive applications. To do so, intrinsically conductive polymers, polypyrrole and PEDOT were used, in order to grant high conductivities to commercially available textiles, lycra and felt. It was determined that the best conditions for polymerization were 3 hours' time for PPy-lycra, 2 hours for PPy-felt and 30 minutes for PEDOT functionalization, as the most economical solution, since polymerization time wasn´t determined to be relevant to the synthesis of PEDOT´s samples.

Morphological characterization was studied, in SEM and Raman. Through scanning electron microscopy fibre orientation is observed, proving unidirectional orientation of course fibres on lycra and lack of organization of fibres in felt textiles. Coating is homogenously observed, and clusters of conductive polymers are present in textiles, concluding that lycra textiles show more clusters between interwoven fibres, while felt sees more aggregation of ICP in superficial fibres. These micron sized structures may actually worsen conductivity. Raman characterization is used to prove and study the existence of PPy and PEDOT on samples, concluding that the most important peaks are present in polymerized textiles.

Piezoresistive behaviour, in combination with course fibre orientation (in lycra) and induced strain through stretching or pressing, is what causes the textiles to work as a sensor. Piezoresistive characterizations were conducted with homemade machines assisted with an Arduino which showed some limitations. In fatigue traction tests (lycra), working ranges and gauge factors were calculated. For polypyrrole samples, these metrics increased with fatigue, showing higher sensitivity and the ability to measure higher ranges of motion, going from a gauge factor of -2.10 to -2.90 , while for PEDOT samples, working ranges slightly increased, translating in higher sensed motions, while gauge factors decreased, from -1.72 to -1.61, meaning less sensitivity of the sensor. In pressure tests (felt), working range, gauge factors and linearity was studied. The textiles performed better in the high threshold of medium pressure regime (90 KPa), than they did for low pressure regimes (15 Pa) as expected, since low pressures are harder to detect for sensors, going from a sensitivity of 1.55 to 2.20 for PPy-felt and 2.15 to 3.05 for PEDOT-felt textiles. Wider working range intervals, higher sensitivity and lower linearities, means the sensors stabilize faster for a wider interval of electrical resistances. Still these metrics alone can´t completely justify sensors 'capabilities, and other important metrics such as hysteresis and responsiveness, the parameters that explain the relaxing of the sensor from a strained state to a relaxed state based on electrical resistance should be carried out in future works.

Finally, stability tests were conducted to understand how textiles would hold on a day-to-day basis if they were used as regular textiles. It´s concluded through conductivities that the conditions of these textiles can be severely degraded in daily operations. Abrasion tests simulated the friction between textile and skin, for a total of 10,200 passages, resulting in a significant decline of conductivity. Felt had the best stability with values from $3.90\text{x}10^{-4}$ S.cm^{-1} to $6.69\text{x}10^{-6}$ S.cm^{-1}, while lycra had the worst results, from $1.24\text{x}10^{-4}$ S.cm^{-1} to $2.70\text{x}10^{-11}$ S.cm^{-1} . Washing cycles were repeated 10 times, simulating a household washing machine. Lycra-PEDOT had the worst results going from $7.25\text{x}10^{-5}$ S.cm^{-1} to $3.99\text{x}10^{-9}$ S.cm^{-1}, while felt-PEDOT had the best results, ranging from $3.91\text{x}10^{-4}$ S.cm^{-1} to $4.57\text{x}10^{-7}$ S.cm^{-1}. Conductivities over time were studied as well, using samples that were kept in storage for 6 months, concluding that conductivities lowered almost 1 order of magnitude.

In sum, an easy to produce method of functionalizing textiles for piezoresistive sensors was achieved. Through use of *in situ* chemical polymerization, two methods are studied to detail. One uses a solution-based mixture, which yields good results but also generate residues, while the other uses a

vapour driven polymerization, resulting in a more homogenous but uncontrolled polymerization, since there doesn´t seem to be any correlation between time of polymerization and conductivity. This means that solution-based polymerizations might lead to higher productions, and so, dopants and surfactants should be studied in order to understand stability of fibres or yarns. The undesirable clusters are also an interesting body of study and a trade-off between how they affect the conductivity of textiles and the work and expanse that is required to see less of these structures is important to achieve for better processability.

Homemade machines assisted with Arduino provided a fast learning curve in more advanced electronics needed to evaluate piezoresistive metrics, but structural problems have also been present. Higher strains of up to 50% in fatigue-traction tests should be studied in future works, therefore an upgrade to 3-D modulated structures using surfaces more capable of fixing textiles without these sliding is pivotal. In future works, Young´s modulus, responsiveness and hysteresis need to be addressed as literature show how fatigue tests which end up with higher working ranges, alter responsiveness of the textile to return to normal electrical resistance when going from a strained to a relaxed state after a high number of cycles. Yarns are also an interesting body of study, as these are capable of being sewn in the textile, having a safe encapsulation from the textile itself.

Stability tests prove that much work is still needed in order for e-textiles to hit a more generalized market, as abrasion through direct contact and washing significantly deteriorates conductivity. Finally, other methods are essential for preserving the textiles capabilities, as these react with atmospheric gases and water, seeing as 6 months was enough to lower almost an order of magnitude in conductivity for all tested textiles. Low-temperature polymerization or plasma treatments could be a solution for high performance and enduring e-textiles.

All these proposals envision a better functional textile that could be used with energy harvesting batteries and has a potential of integration, to signals that can communicate real time piezoresistive metrics to a device such as a computer or smartphone.

References

[1] V. Koncar, “Introduction to smart textiles and their applications,” in *Smart Textiles and Their Applications*, Elsevier Ltd, 2018, pp. 1–8.

[2] L. M. C. Flatau and A. B, “Smart fabric sensors and e-textile technologies : a review,” *Smart Mater. Struct.*, 2014.

[3] Y. Ding, M. A. Invernale, and G. A. Sotzing, “Conductivity trends of pedot-pss impregnated fabric and the effect of conductivity on electrochromic textile,” *ACS Appl. Mater. Interfaces*, vol. 2, no. 6, pp. 1588–1593, 2010.

[4] Shanhong Liu, “Smart clothing unit shipments worldwide from 2016 to 2022 (in millions),” *Statista*, 2019. .

[5] A. Jenkins, P. Kratochvil, R. Stepto, and U. Suter, “International , Union of Pure Glossary of Basic Terms in Polymer,” *Pure Appl. Chem.*, vol. 68, no. 12, pp. 2287–2311, 1996.

[6] A. Elschner, S. Kirchmeyer, W. Lovenich, U. Merker, and K. Reuter, *PEDOT: Principles and application of an Intrinsically Conducting Polymer*. CRC Press, 2010.

[7] A. G. MacDiarmid, “‘Synthetic Metals’: A Novel Role for Organic Polymers,” *J. Am. Stat. Assoc.*, vol. 71, no. 353, p. 252, 1976.

[8] P. Arturo and H. Herrera, “Electrosynthesis and DSC Characterization of Doped Polypyrrole Films with Sodium Salicylate and Sodium Ibuprofen on the Mg Alloy AZ31,” no. August, 2018.

[9] S. W. John, “Synthesis, characterisation and applications of conducting polymer coated textiles,” *Univ. Wollongong Thesis Collect. Model. Control Conduct. Polym. actuators*, 2008.

[10] M. Kesik *et al.*, “Synthesis and characterization of conducting polymers containing polypeptide and ferrocene side chains as ethanol biosensors,” *Polym. Chem.*, vol. 5, no. 21, pp. 6295–6306, 2014.

[11] T. V Vernitskaya and O. N. Efimov, “Polypyrrole : a conducting polymer ; its synthesis , properties and applications,” *Russ. Chem. Rev.*, vol. 66, no. 5, pp. 443–457, 1997.

[12] A. Yussuf, M. Al-saleh, S. Al-enezi, and G. Abraham, “Synthesis and Characterization of Conductive Polypyrrole : The Influence of the Oxidants and Monomer on the Electrical , Thermal , and Morphological Properties,” *Int. J. Polym. Sci.*, vol. 2018, p. 8, 2018.

[13] J. Wu, D. Zhou, C. O. Too, and G. G. Wallace, “Conducting polymer coated lycra,” *Synth. Met.*, vol. 155, no. 3, pp. 698–701, 2005.

[14] X. Cheng *et al.*, “Polypyrrole-coated fabric strain sensor with high sensitivity and good stability,” *Proc. 1st IEEE Int. Conf. Nano Micro Eng. Mol. Syst. 1st IEEE-NEMS*, no. February 2006, pp. 1245–1249, 2006.

[15] A. C. Baptista *et al.*, “Cellulose-based electrospun fibers functionalized with polypyrrole and polyaniline for fully organic batteries,” *J. Mater. Chem. A*, vol. 6, no. 1, pp. 256–265, 2018.

[16] Y. Li, X. Y. Cheng, M. Y. Leung, J. Tsang, X. M. Tao, and M. C. W. Yuen, “A flexible strain sensor from polypyrrole-coated fabrics,” *Synth. Met.*, vol. 155, no. 1, pp. 89–94, 2005.

[17] I. Cucchi, A. Boschi, C. Arosio, F. Bertini, G. Freddi, and M. Catellani, “Bio-based conductive composites : Preparation and properties of polypyrrole (PPy) -coated silk fabrics,” vol. 159, pp. 246–253, 2009.

[18] A. KAYNAK and E. H˚AKANSSON, “Generating Heat from Conducting Polypyrrole-Coated PET Fabrics,” vol. 24, no. 3, pp. 194–207, 2005.

[19] C. L. Heisey, J. P. Wightman, E. H. Pittman, H. H. Kuhn, and S. Carolina, “Surface and Adhesion Properties of Polypyrrole-Coated Textiles,” pp. 247–256, 2015.

[20] K. W. Oh, H. J. Park, and S. H. Kim, “Stretchable conductive fabric for electrotherapy,” *J. Appl. Polym. Sci.*, vol. 88, no. 5, pp. 1225–1229, 2003.

[21] S. H. Chang, C. H. Chiang, F. S. Kao, C. L. Tien, and C. G. Wu, “Unraveling the Enhanced Electrical Conductivity of PEDOT:PSS Thin Films for ITO-Free Organic Photovoltaics,” *IEEE Photonics J.*, vol. 6, no. 4, 2014.

[22] B. Hu, D. Li, P. Calvert, and Q. Fan, “Conductive Textiles via Vapor-Phase Polymerization of,” no. July, 2017.

[23] J. Eom *et al.*, “Highly Sensitive Textile Strain Sensors and Wireless User-Interface Devices Using All-Polymeric Conducting Fibers,” *ACS Appl. Mater. Interfaces*, vol. 9, no. 11, pp. 10190–10197, 2017.

[24] S. Qin, “Textile strain sensors: a review of the fabrication technologies, performance evaluation and applications,” *Mater. Horizons*, no. 6, pp. 219–249, 2018.

[25] J. P. Wang, P. Xue, and X. M. Tao, “Strain sensing behavior of electrically conductive fibers under large deformation,” *Mater. Sci. Eng. A*, vol. 528, no. 6, pp. 2863–2869, 2011.

[26] A. Mirabedini, J. Foroughi, and G. G. Wallace, “Developments in conducting polymer fibres: From

established spinning methods toward advanced applications," *RSC Adv.*, vol. 6, no. 50, pp. 44687–44716, 2016.
[27] Y. Cheng, R. Wang, J. Sun, and L. Gao, "A Stretchable and Highly Sensitive Graphene-Based Fiber for Sensing Tensile Strain, Bending, and Torsion," *Adv. Mater.*, vol. 27, no. 45, pp. 7365–7371, 2015.
[28] X. Liao *et al.*, "A Highly Stretchable ZnO@Fiber-Based Multifunctional Nanosensor for Strain/Temperature/UV Detection," *Adv. Funct. Mater.*, vol. 26, no. 18, pp. 3074–3081, 2016.
[29] X. Wang, X. Fu, and D. D. L. Chung, "Strain sensing using carbon fiber," *J. Mater. Res.*, vol. 14, no. 3, pp. 790–802, 1999.
[30] A. C. H. Rowe, "Piezoresistance in silicon and its nanostructures," *J. Mater. Res.*, vol. 29, no. 6, pp. 731–744, 2014.
[31] P. Costa *et al.*, "Piezoresistive polymer blends for electromechanical sensor applications," *Compos. Sci. Technol.*, 2018.
[32] M. Lu, R. Xie, Z. Liu, Z. Zhao, H. Xu, and Z. Mao, "Enhancement in electrical conductive property of polypyrrole-coated cotton fabrics using cationic surfactant," *J. Appl. Polym. Sci.*, vol. 43601, pp. 1–7, 2016.
[33] W. Rehnby, M. Gustafsson, and M. Skrifvars, "Coating of Textile Fabrics with Conductive Polymers for Smart Textile Applications," no. June 2008, 2013.
[34] J. Singh, M. M. Nayak, and K. Nagachenchaiah, "Linearity and Sensitivity Issues in Piezoresistive Pressure Sensors," *System*, pp. 1–6.
[35] N. Bryan-kinns, "Analysis of Sensitivity, Linearity, Hysteresis, Responsiveness, and Fatigue of Textile Knit Stretch Sensors," *Sensors*, 2019.
[36] N. zdil, G. Zelik, and G. Spren, "Analysis of Abrasion Characteristics in Textiles," in *Abrasion Resistance of Materials*, no. Figure 1, 2012.
[37] S. Garg, C. Hurren, and A. Kaynak, "Improvement of adhesion of conductive polypyrrole coating on wool and polyester fabrics using atmospheric plasma treatment," *Synth. Met.*, vol. 157, no. 1, pp. 41–47, 2007.
[38] A. Kaynak and R. Foitzik, "Methods of Coating Textiles with Soluble Conducting Polymers," *Res. J. Text. Appar.*, 2011.
[39] A. Kaynak and R. Foitzik, "Methods of Coating Textiles with Soluble Conducting Polymers," *Res. J. Text. Appar.*, vol. 15, no. 2, pp. 107–113, 2011.
[40] H. R. Nejad, M. P. Punjiya, and S. Sonkusale, "WASHABLE THREAD BASED STRAIN SENSOR FOR SMART TEXTILE Tufts University , Electrical and Computer Department ," pp. 1183–1186, 2017.
[41] Dejan, "How To Control a Stepper Motor with A4988 Driver and Arduino." [Online]. Available: https://howtomechatronics.com/tutorials/arduino/how-to-control-stepper-motor-with-a4988-driver-and-arduino/.
[42] B. de Bakker, "Force Sensing Resistor (FSR) with Arduino Tutorial." [Online]. Available: https://www.makerguides.com/fsr-arduino-tutorial/.

Appendix A

Appendix A shows information pertinent to designed acetate masks, using silhouette studios software and hardware in order to produce high mm precision for in-plane conductivity tests. Figure A.0.1 shows the design of masks.

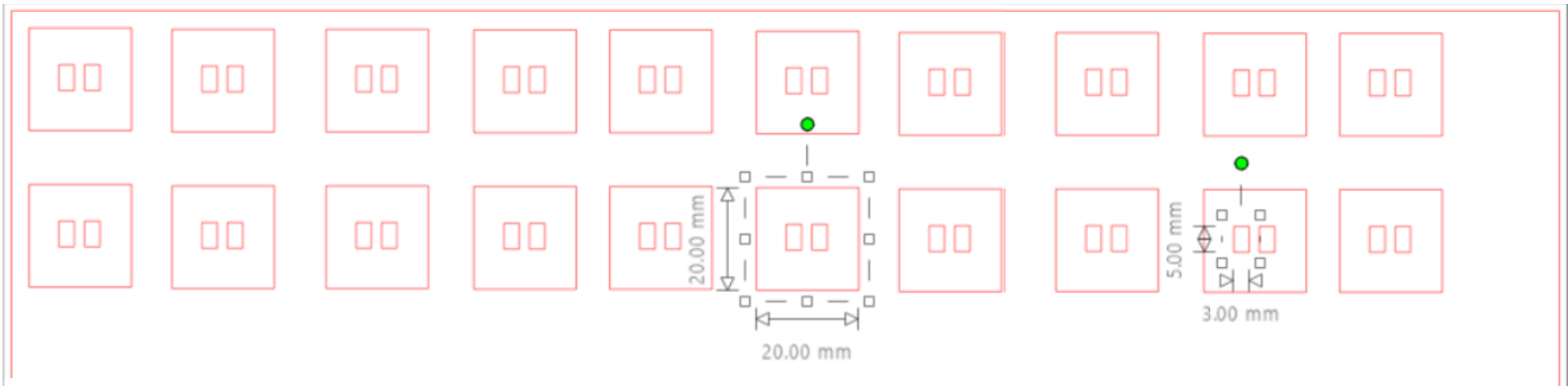

Figure A.0.1- Image of designed acetate masks and dimensions using silhoutte studios.

Masks were designed with a 2.0x2.0cm on the outside borders and a 3.0x5.0mm usable area to paint the soluble carbon ink contacts.

The masks showed great precision. A coating of carbon ink was done with a metallic spatula and left to dry at ambient temperature (25℃) before removing the mask. The dimensions of the contacts were examined after and used for calculating conductivity values, described in equation 3.2, where L is the distance between contacts, and d is the length of contacts.

Appendix B

Appendix B shows some EDS results that unfortunately were not included in the main body of work since there weren´t results present for all tested textiles.

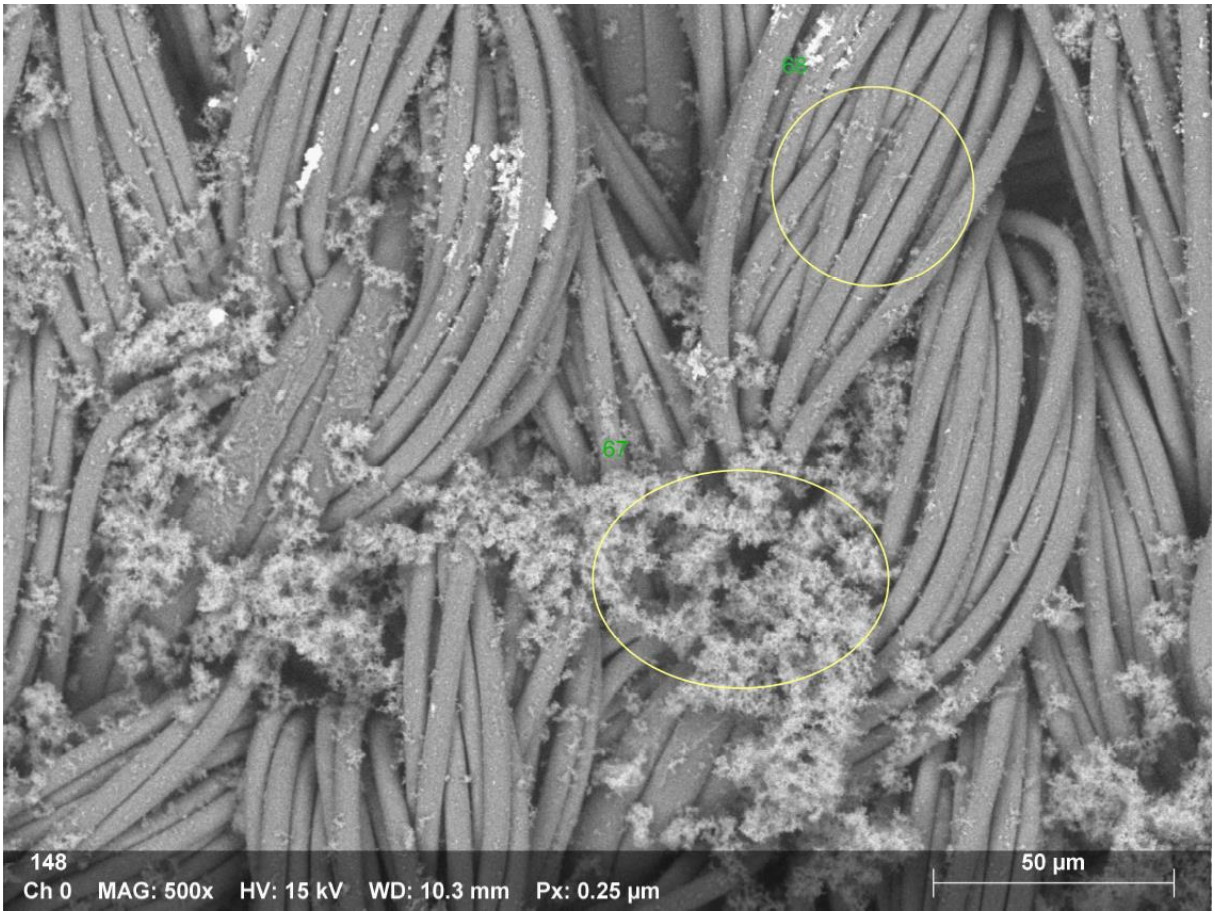

Figure B0. 1-SEM image of lycra-PPy and identified clusters.

Table B.0. 1-Chemical composition of identified cluster in lycra-PPy.

67

Element	At. No.	Netto	Mass [%]	Mass Norm. [%]	Atom [%]	abs. error [%] (1 sigma)	rel. error [%] (1 sigma)
C	6	88272	59.41	59.41	65.88	6.77	11.39
O	8	14717	18.97	18.97	15.79	2.55	13.43
N	7	5948	17.73	17.73	16.86	2.72	15.33
Cl	17	29206	3.89	3.89	1.46	0.16	4.05
		Sum	**100.00**	**100.00**	**100.00**		

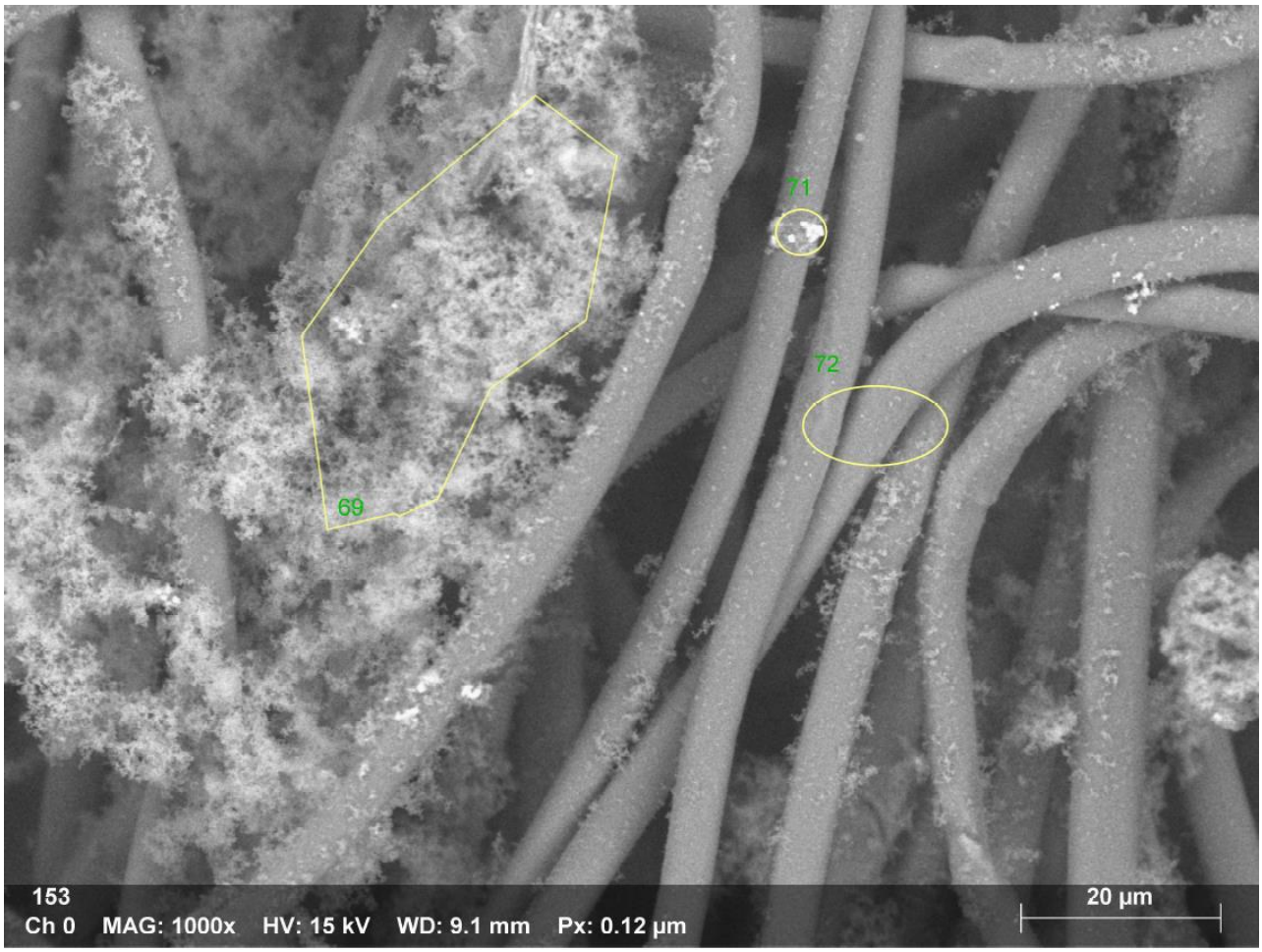

Figure B0. 2-SEM image of felt-PPy and identified clusters.

Table B.0. 2-Chemical composition of identified clusters in felt-PPy.

Normalized mass concentration [%]

Spectrum	C	N	O	Cl	K	Fe
69	59.02	19.91	17.41	3.66		
71	64.95	11.49	15.28	6.86	1.00	0.43
72	65.35	10.11	20.76	3.17		0.62
Mean	**63.11**	**13.84**	**17.81**	**4.56**	**1.00**	**0.52**
Sigma	**3.54**	**5.31**	**2.76**	**2.00**	**0.00**	**0.13**
SigmaMean	**2.05**	**3.06**	**1.60**	**1.16**	**0.00**	**0.08**

Figure B0. 1 and Figure B0. 2 represent SEM images of PPy prepared lycra and felt textiles respectively. Table B.0. 1 and Table B.0. 2 are values given by EDS characterization, in which the presence of Carbon, Nitrogen, Oxygen and Chlorine are observed. This makes sense when observing the reaction formula present in the oxidation of pyrrole via iron (III) chloride:

$$n\ C_4H_2NH + 2n\ FeCl_3 \rightarrow (C_4H_2NH)_n + 2n\ FeCl_2 + 2n\ HCl$$

It´s therefore understandable the abundance of these chemical elements. $FeCl_2$ does not seem to be present, because of washing of by-products. The clusters are usually made of polypyrrole and oxygen present in water.

Figure B0. 3 shows a detailed SEM image of lycra-PEDOT, while *Figure B0. 5* describes the intensity of the found chemical elements. Figure B0. 4 shows a detailed SEM image of felt-PEDOT, and Figure B0. 6 describes the intensity of the found chemical elements.

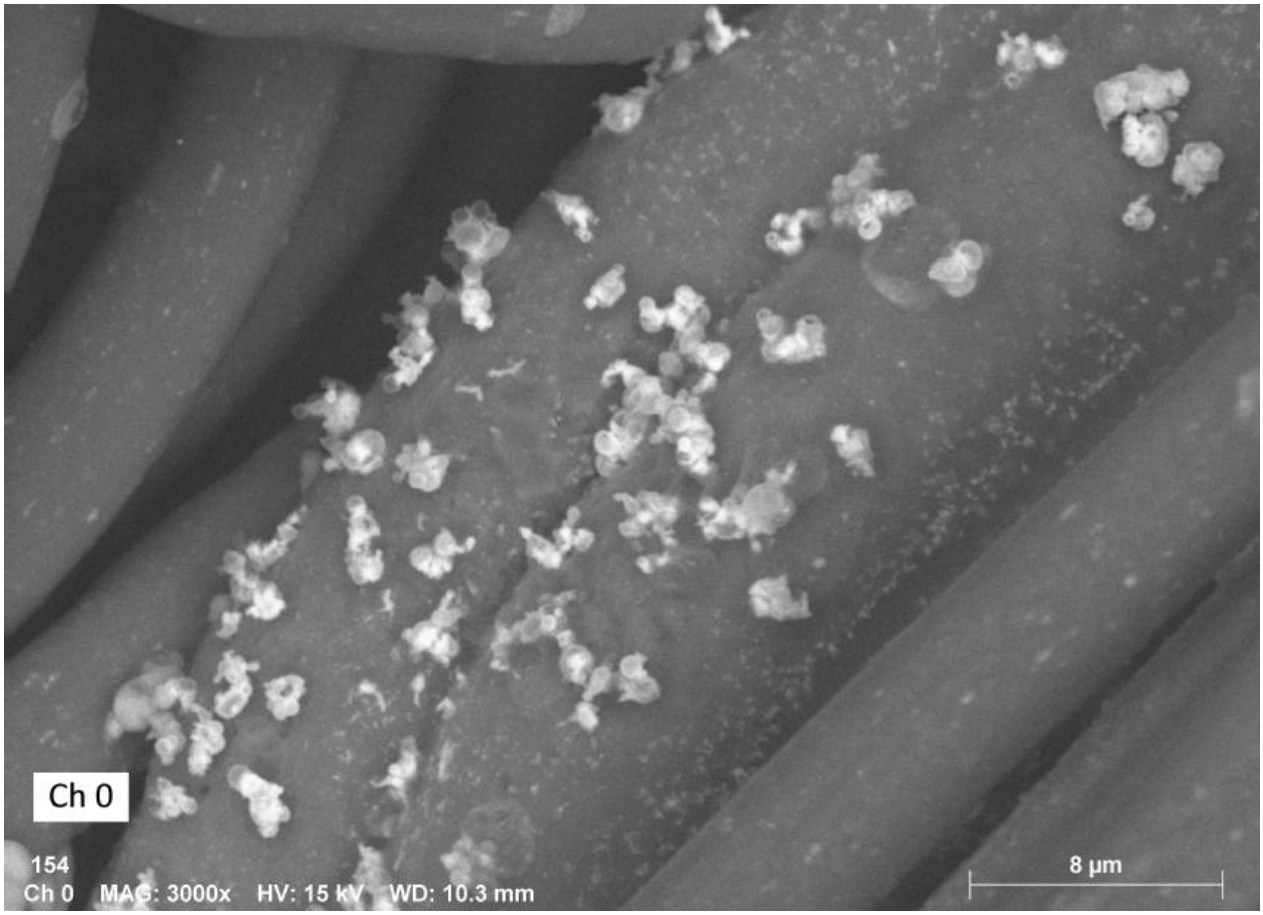

Figure B0. 3-SEM image of lycra-PEDOT.

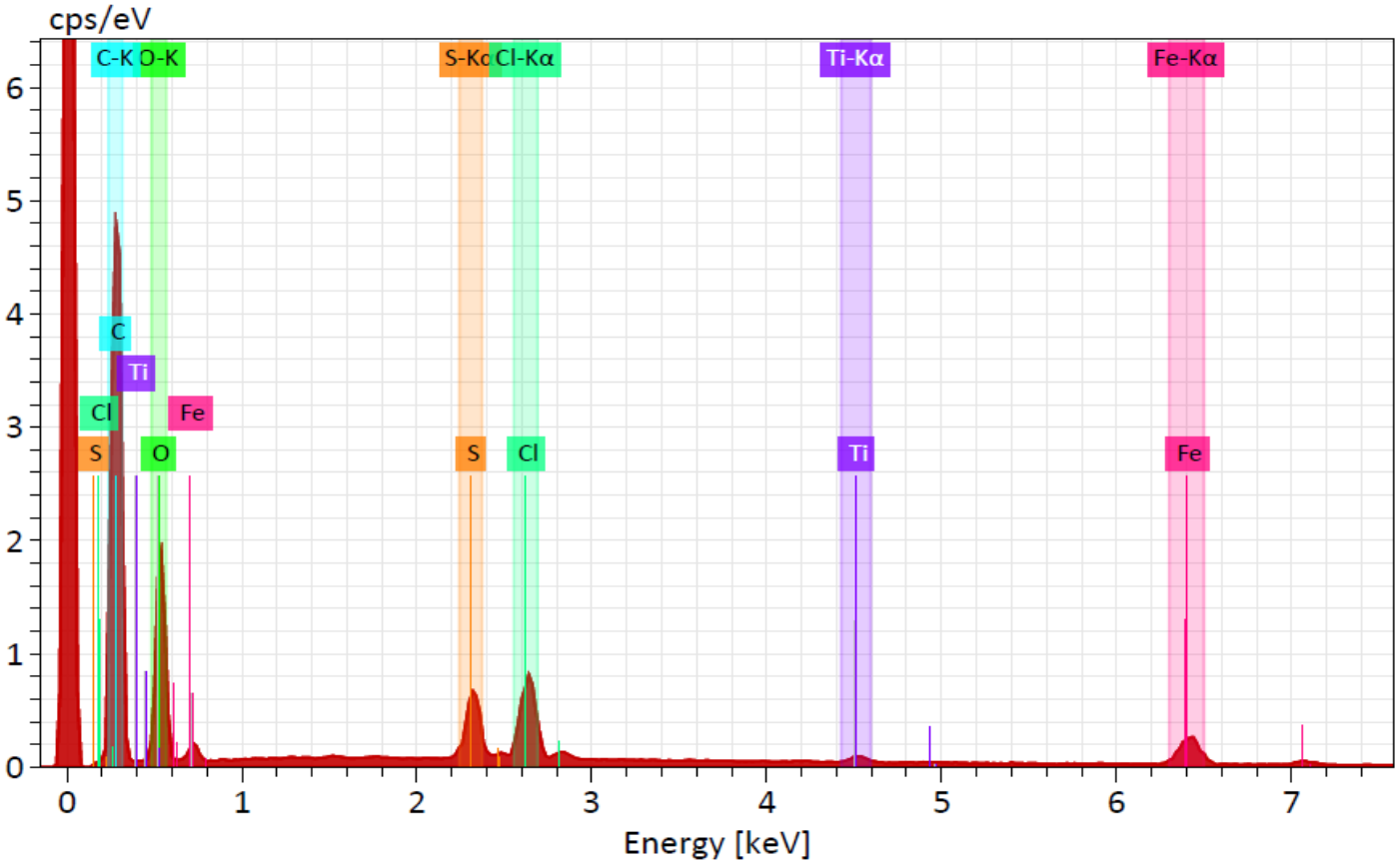

Figure B0. 5-EDS assisted identification of chemical elements for lycra-PEDOT.

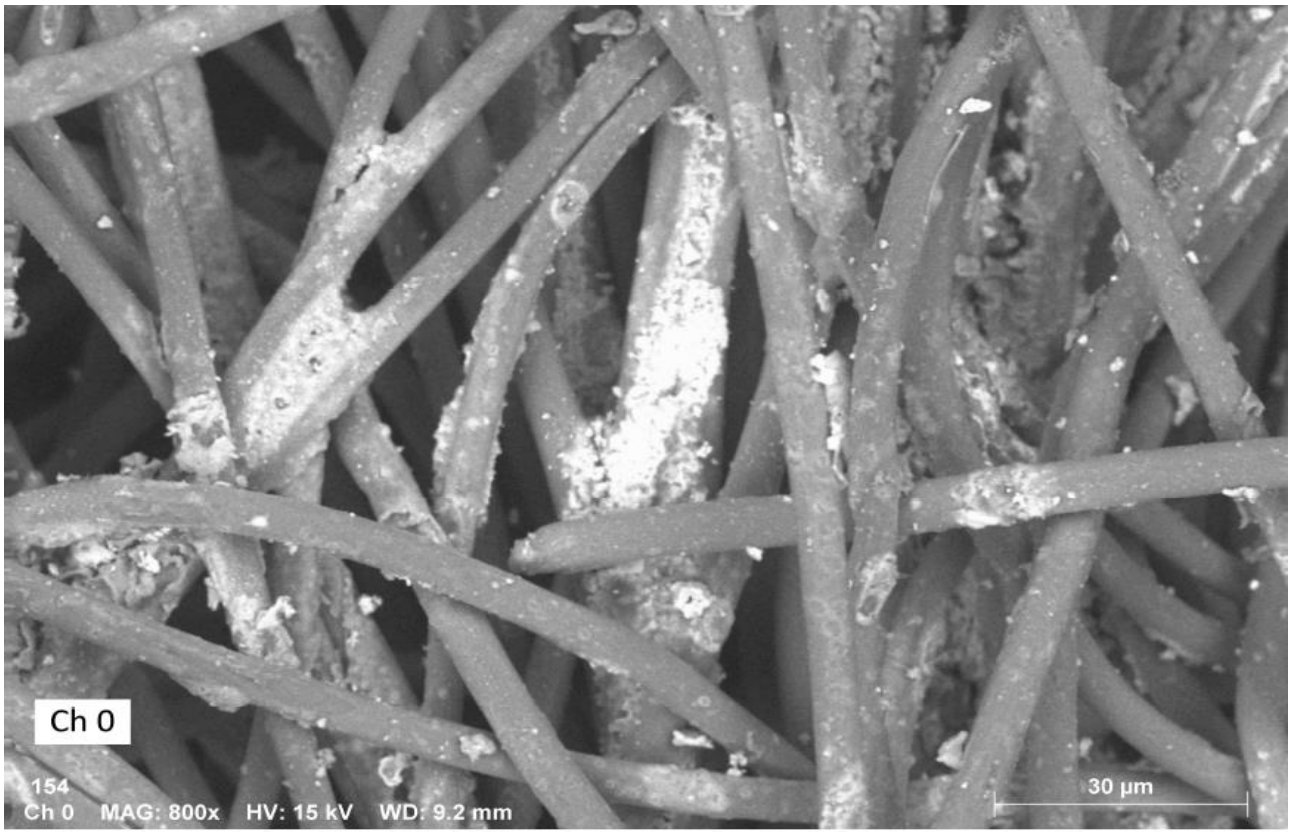

Figure B0. 4-SEM image of felt-PEDOT.

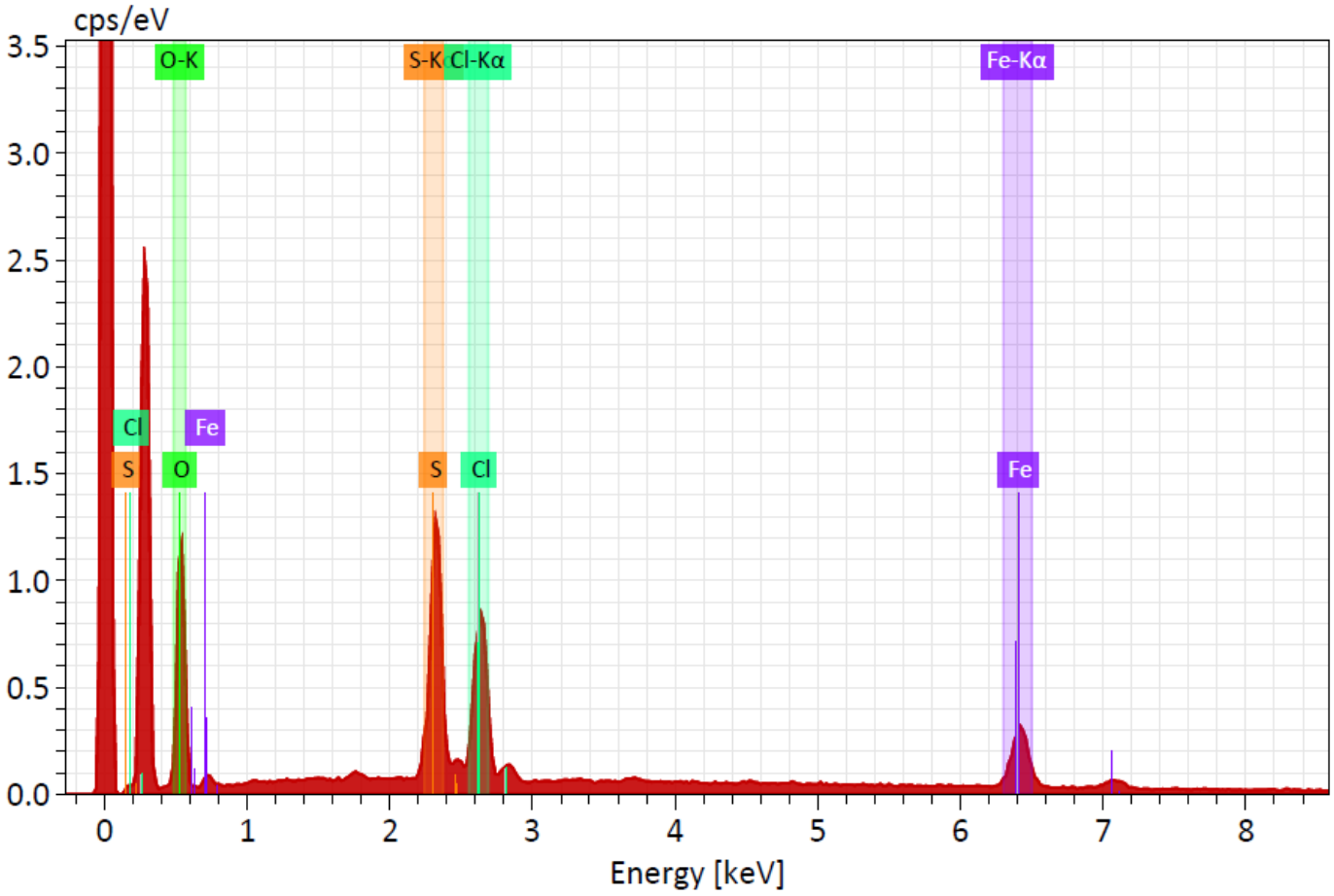

Figure B0. 6-EDS assisted identification of chemical elements for felt-PEDOT.

Appendix C

Appendix C shows information related to the homemade traction machine. Figure C0. 1 shows the main components used from an electronic schematic approach. An Arduino Uno is connected to a breadboard that receives 2 inputs: a 5V input from Arduino and a 12V power source input to feed a stepper motor, controlling the rotations and distance. The driver is then connected to an output in Arduino that checks if the coaxial movement of the stepper is in order, converting that movement to an unidirectional traction movement and therefore deformation of the textile. Wire connections are set to each extremity of the textile, in order to measure electrical resistance in real time, to study fatigue-traction tests in page 19.

The overall schematic was taken from an open source website with more information on traction mechanics [41].

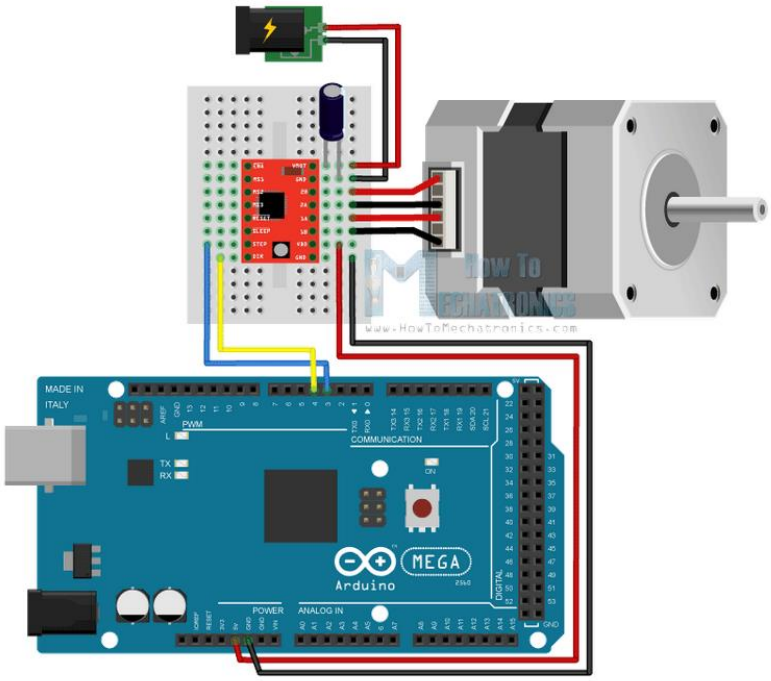

Figure C0. 1-Schematic of main components of traction machine.

A 4 page code with included commentaries that explain part of the code and give some additional information, such as being able to print the rotations in radians are contained in Figure C0.2.

```
//#include <SPI.h>
//#include <SD.h>
//File myFile;
//int pinCS = 53;
#define SM_DIRECTION_PIN         2
#define SM_STEP_PIN              3
#define SM_ENABLE_PIN            4
#define STEPS_PER_REV            250
#define distance                 5
#define EXPERIMENT_REPETITIONS    10
#define RESISTANCE_NUMBER        4
#define RESISTANCE_VALUES        {3300.0,10000.0,20000,100000}
#define RESISTANCE_PINS          {5,6,7,8}
int   L = 3;
float z = 0;
//This lenght is cm

bool finished;
double getResistance()
{
 double read_values[RESISTANCE_NUMBER];
 double resistance_values[RESISTANCE_NUMBER] = RESISTANCE_VALUES;
 byte resistance_pins[RESISTANCE_NUMBER] = RESISTANCE_PINS;

 for (int i = 0; i < RESISTANCE_NUMBER; i++)
 {
   for (int j = 0; j < RESISTANCE_NUMBER; j++)
   {
     pinMode(resistance_pins[j], INPUT);
   }
   pinMode(resistance_pins[i],OUTPUT);
```

Figure C0.2-Condessed fatigue-traction Arduino code.

Appendix D

Appendix D shows information related to the homemade pressure machine. shows the main components used from an electronic schematic approach. An Arduino is connected to a breadboard that receives a 5V input and gives an output based on the voltage measured that is converted to electrical resistance values by using a voltage divider.

In Figure D.0.1 a force sensitive resistor (FSR) is depicted, as these are commercially available piezoresistive sensors used for learning how to work with piezoresistive sensors on open code websites, with the intent of testing and calibrating [42].

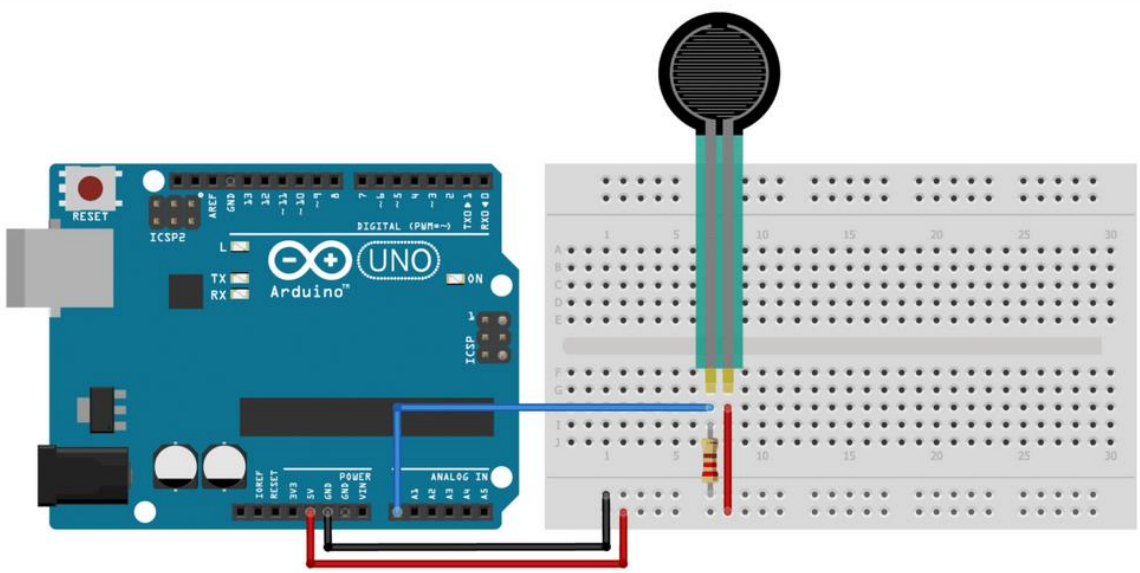

Figure D.0.1-Overall schematic of FSR using an arduino.

The condensed code used with an Arduino Uno is described in Figure D.0.2 with included commentaries on how electrical resistance is measured and calibrated. The code was tinkered with using an open source website [42]. A voltage passes through the thickness of a textile and the difference in input and output of voltage is converted to resistance changes.

Figure D.0. 3 shows the end design and working function of a homemade pressure machine using Catia V5 software. The textile is put between the support structure and pressed with controlled force in order to measure a differential in electrical resistance seen in pressure tests in page 22.

```
/* FSR testing sketch.

Connect one end of FSR to power, the other end to Analog 0.
Then connect one end of a 10K resistor from Analog 0 to ground

int fsrPin = 0;     // the FSR and known pulldown are connected to a0
int fsrReading;     // the analog reading from the FSR resistor divider
int fsrVoltage;     // the analog reading converted to voltage
unsigned long fsrResistance;  // The voltage converted to resistance, can be very big so make "long"
unsigned long fsrConductance;
long fsrForce;      // Finally, the resistance converted to force

void setup(void) {
 Serial.begin(9600);   // We'll send debugging information via the Serial monitor
 //Serial.println("Time;Resistance;Conductance;Force");
}

void loop(void) {
 fsrReading = analogRead(fsrPin);
 //Serial.print("Analog reading = ");
 //Serial.println(fsrReading);

 // analog voltage reading ranges from about 0 to 1023 which maps to 0V to 5V (= 5000mV)
 fsrVoltage = map(fsrReading, 0, 1023, 0, 5000);
 //Serial.print("Voltage reading in mV = ");
 //Serial.println(fsrVoltage);

 Serial.print(millis());
 Serial.print(";");
 if (fsrVoltage == 0) {
   //Serial.println("No pressure");
 } else {
```

Figure D.0.2-Condensed Arduino code used for pressure tests.

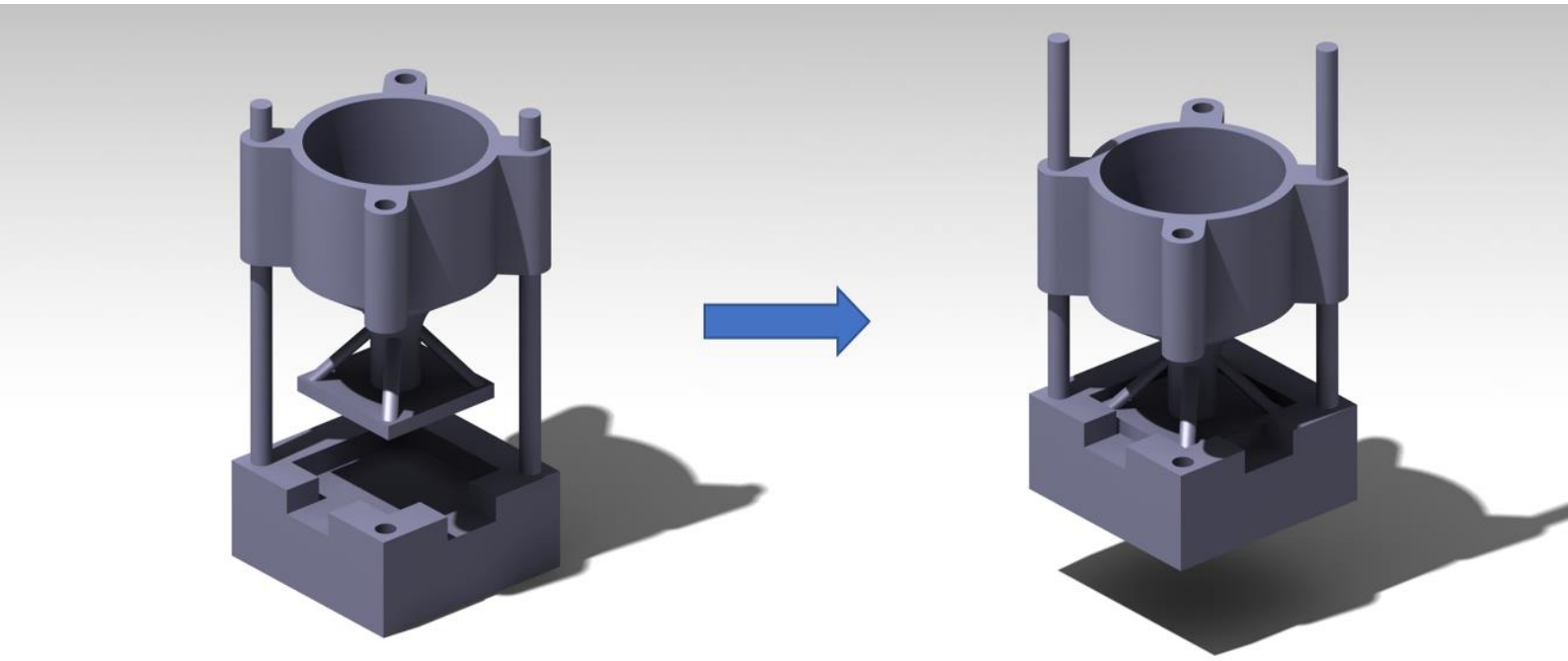

Figure D.0. 3-Design of homemade pressure machine using 3-D modeling.